ROSETTA
Magnetometerexperiment
Missionsphase
FK: 50QP 0402

Abschlußbericht
vorgelegt von

Hans-Ulrich Auster, Karl-Heinz Glaßmeier
und Ingo Richter

Juni 2010

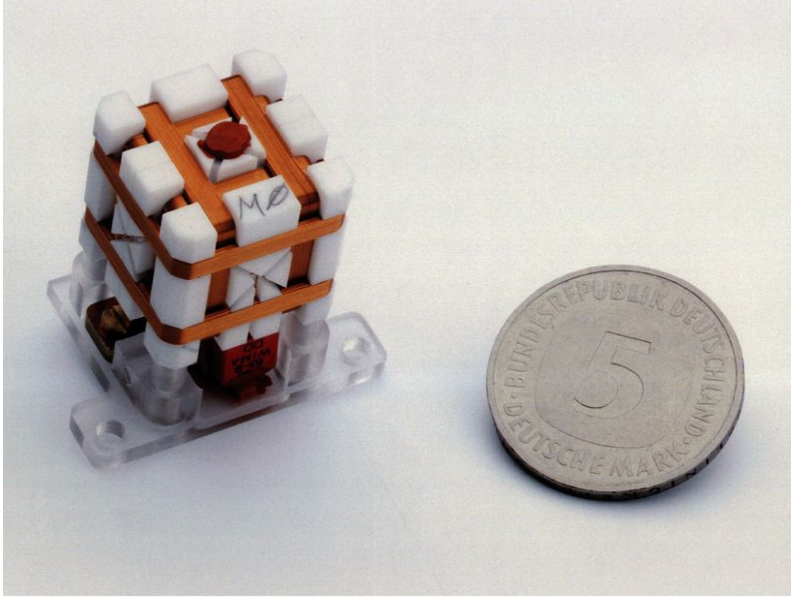

Der RPC-Fluxgate-Magnetometersensor
auf dem
ROSETTA Orbiter
und

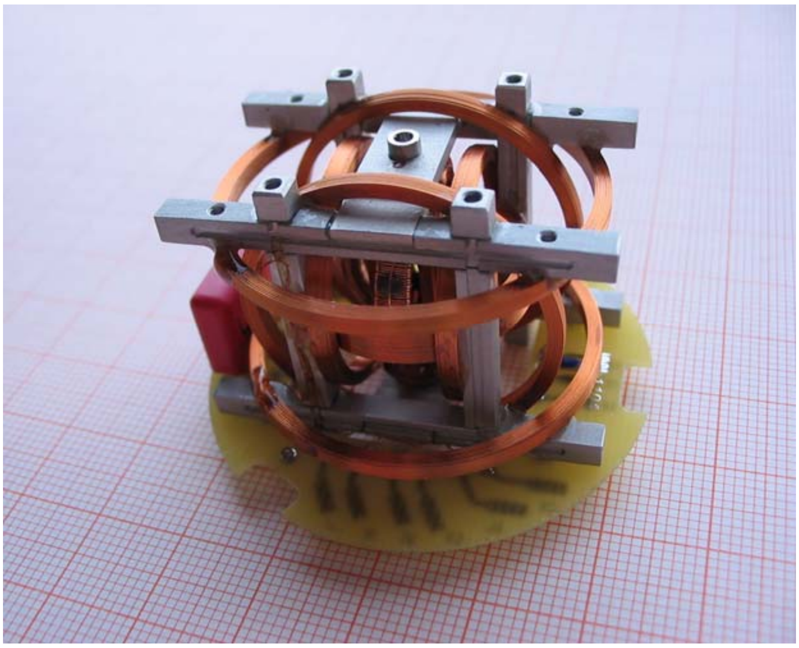

der ROMAP Magnetometersensor des
ROSETTA Landers PHILAE

Inhaltsverzeichnis

1. Einführung

Die ROSETTA-Mission ist eine Cornerstone-Mission der europäischen Weltraumorganisation ESA im Rahmen ihres Horizon 2000 Programms. Ziel dieser extrem ehrgeizigen Mission ist die Erforschung eines Kometen durch eine Raumsonde, die einen Kometenkern über längere Zeit umkreisen soll und durch ein Landegerät, das an der Oberfläche des Kometenkernes wissenschaftliche Messungen durchführen soll.

Eine detaillierte Beschreibung dieses Projektes geben Glassmeier et al. (2007) und Schulz et al. (2009) (siehe **Anlagen A und B**). An Bord des ROSETTA Orbiters und des ROSETTA Landers PHILAE befinden sich Fluxgate Magnetometerexperimente, die unter der Leitung von K.H. Glaßmeier (PI RPC-Mag) und H.U. Auster (PI ROMAP) am Institut für Geophysik und extraterrestrische Physik der Technischen Universität Braunschweig entwickelt wurden und nach dem erfolgreichen Start der ROSETTA-Sonde 2004 im Rahmen des Forschungsvorhabens „ROSETTA Magnetometer: Missionsphase“ wissenschaftlich betreut wurden.

Das ROSETTA Orbiter Magnetometer (Instrument Manager I. Richter) ist Teil des ROSETTA Plasma Consortium (RPC), das aus den folgenden Sensoren besteht:

-	MAG:	Fluxgate Magnetometer Sensor	PI: K.H. Glassmeier, Braunschweig
-	LAP:	Langmuir Probe	A. Eriksson, Uppsala
-	MIP:	Mutual Impedance Probe	J. G. Trotignon, Orleans
-	IES:	Ion-Electron Spectrometer	J. Burch, San Antonio
-	ICA:	Ion Composition Analyser	R. Lundin, Kiruna
-	PIU:	Plasma Interface Unit	C. Carr, London

Das Rosetta Lander Magnetometer ist Teil des ROMAP Experimentes, das aus folgenden Sensoren besteht:

-	MAG:	Fluxgate Magnetometer	PI: H.U. Auster, Braunschweig
-	SPM:	Simple Plasma Monitor	I. Apathy, Budapest

2. Wissenschaftliche Zielsetzung

Das hauptsächliche Ziel der wissenschaftlichen Messungen des Fluxgate Magnetometers des ROSETTA Plasmainstrumentes ist das Studium der Wechselwirkung zwischen dem magnetisierten Sonnenwindplasma und dem Kometen P/Churyumov-Gerasimenko während der Annäherung des Kometen an die Sonne. Im Vordergrund steht dabei die Frage der Veränderung dieser Wechselwirkung in Abhängigkeit von der kometaren Aktivität. Ein weiteres wesentliches Ziel der Magnetometerexperimente ist die Untersuchung etwaiger magnetischer Materialien an der Kometenoberfläche sowie die Untersuchung von Induktionseffekten, die Rückschlüsse auf das Kometeninnere zulassen.

Zur Vorbereitung dieser wissenschaftlichen Ziele sind umfangreiche Testphasen vorgesehen. Vor dem Erreichen des Kometen im Jahre 2014 wird ROSETTA eine Reihe von Planeten- und Asteroidenvorbeiflügen absolvieren, die einerseits eine detaillierte Überprüfung der Funktionsfähigkeit des Fluggerätes erlaubt, andererseits interessante wissenschaftliche Untersuchungen an den besuchten Objekten ermöglicht. Folgende Vorbeiflüge und Missionsphasen sind geplant:

März 2005:	1. Erdvorbeiflug
März 2007:	Mars-Vorbeiflug
November 2007:	2. Erdvorbeiflug
September2008:	Asteroidenvorbeiflug (Steins)
November 2009:	3. Erdvorbeiflug
Juli 2010:	Asteroidenvorbeiflug (Lutetia)
Juli 2011:	Beginn der Überwinterung
Januar 2014:	Aufwachen aus dem Winterschlaf
Mai 2014:	Rendevous
November 2014:	Landung auf dem Kometen
August 2015:	Perihel-Durchgang
Dezember 2015:	Missionsende

Im Rahmen dieses Vorhabens wurden insbesondere die Erdvorbeiflüge, der Marsvorbeiflug und der Vorbeiflug am Asteroiden Steins technisch-wissenschaftlich betreut. Weitere Einzelheiten der wissenschaftlichen Zielsetzung und ihrer möglichen Umsetzung sind den Experimentbeschreibungen von Glassmeier et al. (2007) und Auster et al. (2007) zu entnehmen (**Anlagen C und D**).

3. Instrumentbeschreibung

Das für den ROSETTA Orbiter entwickelten Magnetometer sind sogenannte Fluxgate-Magnetometer, wie es bei vielen Satellitenmissionen zum Einsatz gekommen ist. Weitere Details zu den Magnetometerexperimenten entnehme man Glassmeier et al. (2007) und Auster et al. (2007) (**Anlagen C und D**) sowie der Beschreibung des PIU- Moduls (Carr et al., 2007; **Anlage E**).

4. ROSETTA Missionsbuch, RPC User-Manual und Archivierung

Im Frühjahr 2009 ist das ROSETTA Missionsbuch veröffentlicht worden (**Anlage B**). In der Erstellung dieses grundlegenden Werkes über die ROSETTA Mission ist der Leiter dieses Vorhabens maßgeblich beteiligt gewesen.

Der Instrumentmanager des RPC-Magnetometerexperimentes, I. Richter, ist im Rahmen der Aufgabenverteilung innerhalb des RPC Consortiums für die Pflege und Erweiterung des RPC User-Manuals verantwortlich gewesen. Das UM ist während der kompletten Mission **das** maßgebliche Dokument zur Bedienung des RPC- Experimentes:

- Es enthält eine komplette Experimentbeschreibung inklusive technischer Daten, Zeichnungen und technischer Details, auf die bei Bedarf zurückgegriffen werden kann.
- Im UM sind die Interfaces zum S/C inklusive Kommandos, Parameter, Timing usw. beschrieben.
- Die komplette Struktur der Telemetriepakete und der Telekommandos kann dem UM entnommen werden.
- Es wird zur quantitativen Analyse von Leistungs– u. Telemetriebudgetabschätzungen zu Rate gezogen.

- Es wird zur Planung einzelner Missionsphasen benutzt, da das UM das einzige Dokument ist, in dem alle Messmodi jedes Experimentes detailliert beschrieben sind.
- Alle relevanten Testprozeduren, sowohl für die Boden- als auch für die „in Flight" Tests, sind im UM beschrieben.
- In Falle eines aufgetretenen Fehlers können die im UM definierten Notprozeduren aktiviert werden.
- Der Thermalhaushalt ist im UM dokumentiert und kann bei thermischen Ausnahmesituationen zur Problemlösung herangezogen werden.
- Das UM enthält eine Referenz auf die komplette ROSETTA Datenbank (RSDB), in der alle zum Betrieb von RPC benutzten Kommandos, Parameter und Variablen definiert sind.
- Eine Referenz auf alle Flight Control Procedures (FCPs) und On board Control Procedures (OBCPs) ist vorhanden.
- Das UM enthält ein ausgedehntes ESA Akronymverzeichnis, das das tägliche Arbeiten und die Kommunikation mit dem Projekt erheblich vereinfacht.

Das UM wurde während der Experimentintegrationsphase initiiert und wird fortlaufend auch während der aktiven Mission bei Bedarf ständig aktualisiert, so dass RPC-Team stets auf eine gültige Dokumentation zurückgreifen kann. Eine aktuelle Version findet sich in der **Anlage F.**

Bei einem so umfangreichen Projekt, wie es ROSETTA darstellt, ist eine umfängliche Archivierung unerlässlich. Die Archivierung beinhaltet dabei sowohl

- Kenntnisse und Details, die beim Bau des Magnetometers zur Anwendung kamen,

als auch

- die Speicherung und Verarbeitung der gewonnenen Daten während der Mission.

Im Rahmen dieses Vorhabens wurden umfangreiche Beiträge zur Archivierung der bisherigen Daten der Magnetometer- und Plasmainstrumente sowie zum grundsätzlichen Aufbau des Archivs geleistet.

Die Kommandierung, Datenverarbeitung und Analyse sowie die Archivierung des Experimentes ROMAP erfolgte wie für alle Landerexperimente unter Schirmherrschaft des Science Operation and Navigation Center (SONC) in Toulouse und des Lander Control Center (LCC) in Köln. Hierzu wurden in Zusammenarbeit mit SONC und LCC folgende Dokumente erarbeitet:

- ein Experiment Archive Interface Control Document (EAICD) (**Anlage M**)
- eine WEB basierende Software zum Datenzugriff und zur Datenvisualisierung
- die Kommandierung des Experimentes im Rahmen des Flight Operation Plans
- Reports für LCC / SONC für jede der Messkampagnen

5. Erdvorbeiflüge

Um den 1. März 2005, 13. November 2007 und 13. November 2009 hat ROSETTA seine drei geplanten Vorbeiflüge an der Erde durchgeführt. Bei dieser Gelegenheit wurden umfangreiche Testmessungen beider Instrumente durchgeführt und die Ergebnisse miteinander verglichen. Ergebnisse des ersten Vorbeifluges sind z.B. in Glassmeier et al. (2007) dokumentiert. Vollständige Dokumentationen finden sich in den **Anlagen G1-3.**

6. Marsvorbeiflug

Am 25. Februar 2007 ist die ROSETTA Sonde am Mars vorbeigeflogen. **Anlage H** liefert weitere Details der dort durchgeführten Messungen. Die wissenschaftliche Auswertung dieser Beobachtungen lieferte eine Reihe interessanter Ergebnisse, die von Bößwetter et al. (2009) (**Anlage I**) und Edberg et al. (2009) (**Anlage J**) publiziert wurden.

7. Vorbeiflug am Asteroiden Steins

Am 5. September 2008 ist ROSETTA am Asteroiden Steins vorbeigeflogen. **Anlage K** liefert weitere Details der dort durchgeführten Messungen. Die wissenschaftliche Auswertung der gewonnenen Daten erlaubte es, eine obere Grenze für die Magnetisierung dieses Himmelskörpers zu liefern. Details sind in der Publikation Auster et al. (2010) dargestellt, die von der Zeitschrift Planet. Space Sci. zur Veröffentlichung angenommen wurde (**Anlage L**).

8. Anhänge

Die Anlagen beinhalten weitere, im Text erwähnte, ausführliche Informationen zu den Magnetometerexperimenten der ROSETTA Mission. Aus Copyrightgründen sind die wissenschaftlichen Artikel in dieser Berichtsversion nicht beigefügt, sondern werden nur anhand ihrer bibliographischen Angaben gelistet:

Auster, H.U., I. Apathy, G. Berghofer, A. Remizov, R. Roll, K.H. Fornacon, K.H. Glassmeier, G. Haerendel, I. Hejja, E. Kührt, W. Magnes, D. Moehlmann, U. Motschmann, I. Richter, H. Rosenbauer, C.T. Russell, J. Rustenbach, K. Sauer, K. Schwingenschuh, I. Szemerey, R. Waesch, ROMAP: ROSETTA Magnetometer and Plasma Monitor, Space Sci. Rev., 128, 221-240, 2007.

Carr, C.M., E. Cupido, C.G.Y. Lee, A. Balogh, T. Beek, J.L. Burch, C.N. Dunford, A.I. Eriksson, R. Gill, K.H. Glassmeier, R. Goldstein, D. Lagoutte, R. Lundin, K. Lundin, B. Lybekk, J.L. Michau, G. Musmann, H. Nilsson, C. Pollock, I. Richter, J.G. Trotignon, RPC: The Rosetta Plasma Consortium, Space Sci. Rev., 128, 629-647, 2007.

Glassmeier, K.H., I. Richter, A. Diedrich, G. Musmann, U. Auster, U. Motschmann, A. Balogh, C. Carr, E. Cupido, A. Coates, M. Rother, K. Schwingenschuh, K. Szegö, B. Tsurutani, RPC-MAG: The Fluxgate Magnetometer in the ROSETTA Plasma Consortium, Space Sci. Rev., 128, 649-670, 2007.

Glassmeier, K.H., H. Boehnhardt, D. Koschny, E. Kührt, I. Richter, The ROSETTA Mission: Flying towards the Origin of the Solar System, Space Sci. Rev., 128, 1-21, 2007.

Russell, C.T., K.H. Glassmeier, and H. Boehnhardt, Rosetta: Mission to comet 67P/Churyumov-Gerasimenko – Foreword, *Space Sci. Rev.*, 128, 1-4, 2007.

Russell, C. T., K. H. Glassmeier, H. Boehnhard (Eds.), ROSETTA : Mission to Comet 67P/Churyumov-Gerasimenko, Space Science Review, Springer, New York, 2007.

Schulz, R., C. Alexander, H. Boehnhard, K.H. Glassmeier (Eds.), Rosetta: Mission to Comet 67P/Churyumov-Gerasimenko, Springer-Verlag, Heidelberg, 2008.

Edberg, N. J. T., Auster, U., Barabash, S., Bößwetter, A., Brain, D. A., Burch, J. L., Carr, C. M., Cowley, S. W. H., Cupido, E., Duru, F., Eriksson, A. I., Fränz, M., Glassmeier, K. H., Goldstein, R., Lester, M., Lundin, R., Modolo, R., Nilsson, H., Richter, I., Samara, M., Trotignon, J. G., Rosetta and Mars Express observations of the influence of high solar wind pressure on the Martian plasma environment, Ann. Geophys., 27, 4533-4545, 2009.

Boesswetter, A., Auster, U., Richter, I., Fränz, M., Langlais, B., McKenna-Lawlor, S., Simon, S., Motschmann, U., Glassmeier, K. H., Edberg, N. J. T., Lundin, R., Rosetta swing-by at Mars - an analysis of the ROMAP measurements in comparison with results of 3-D multi-ion hybrid simulations and MEX/ASPERA-3 data, Ann. Geophys., 27, 2383-2398, 2009.

Edberg, N. J. T., Eriksson, A. I., Auster, U., Barabash, S., Bößwetter, A., Carr, C. M., Cowley, S. W. H., Cupido, E., Fränz, M., Glassmeier, K. H., Goldstein, R., Lester, M., Lundin, R., Modolo, R., Nilsson, H., Richter, I., Samara, M., Trotignon, J. G., Simultaneous measurements of Martian plasma boundaries by Rosetta and Mars Express, Planet. Space Sci., 57, 1085-1096, 2009.

Anlage A

Anlage B

ROSETTA

ESA's Mission to the Origin of the Solar System

Rita Schulz
Claudia Alexander
Hermann Boehnhardt
Karl-Heinz Glassmeier
Editors

ROSETTA: ESA's Mission to the Origin of the Solar System is the first book on the ESA's Planetary Cornerstone Rosetta Mission, that discusses the science and instrumentation involved. Comets consist of the most primitive material in the solar system. An in depth study of this material could provide us with the knowledge to understand the earliest epoch of the solar system's formation. Until now, our knowledge of comets has come from Earth-based telescopes. and fly-by missions Rosetta will be the first ever spacecraft to rendezvous with a comet, go in orbit around the nucleus. it will stay there for over one year, in order to study the comet's evolution. Rosetta will also land on the surface of the comet with its Lander Philae to perform dedicated in-situ analysis of the comet nucleus composition and structure. The Rosetta mission is an ambitious one that is poised to make a dramatic advance in our understanding of comets, and the origin of our solar system.

ROSETTA: ESA's Mission to the Origin of the Solar System is partially reprinted, with updates and corrections, from *Space Science Reviews Journal*, Vol. 128/1–4, 2007. This book is appropriate for researchers as well as graduate students working in astronomy, planetology, and astrobiology.

ISBN 978-0-387-77517-3
EAN
9 780387 775173 >

>springer.com

Schulz
Alexander
Boehnhardt
Glassmeier
Editors

ROSETTA
ESA's Mission to the Origin of the Solar System

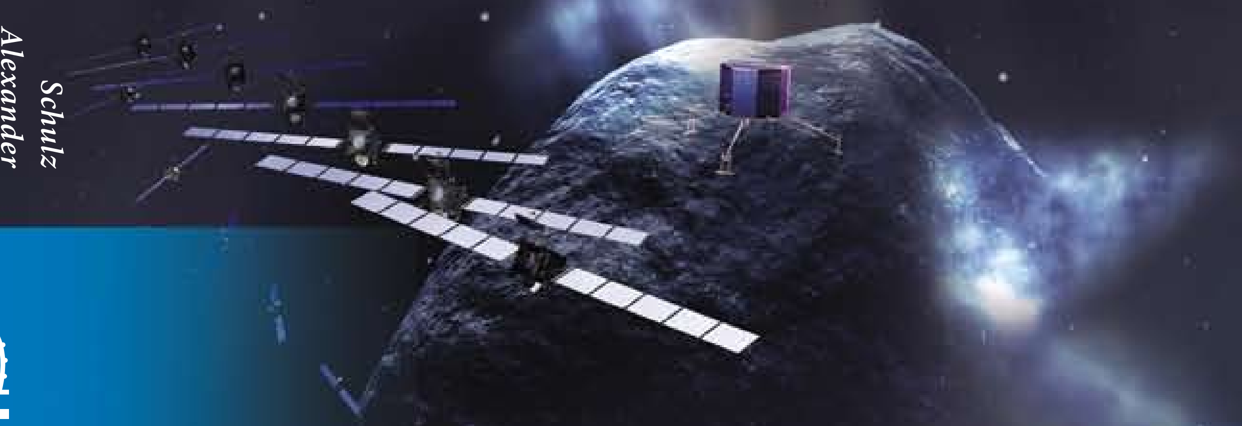

ROSETTA

ESA's Mission to the Origin of the Solar System

Rita Schulz
Claudia Alexander
Hermann Boehnhardt
Karl-Heinz Glassmeier
Editors

Springer

Anlage C

Anlage D

Anlage E

Anlage F

IGEP
TU Braunschweig
Institut für Geophysik und extraterrestrische Physik

ROSETTA PLASMA CONSORTIUM USERS' MANUAL

RO-RPC-UM

Issue 2.12

September 7, 2007

Prepared by:
Ingo Richter (MAG-TM)
Emanuele Cupido-(RPC-TM)

Anlage G1

R O S E T T A

FLIGHT REPORTS
of RPC–MAG

RO–IGEP–TR–0014

Issue: 3 Revision: 0

January 25, 2010

Report of the

First Earth Swing by (EAR1)

Time period: March 01 - 07, 2005

Andrea Diedrich
Karl-Heinz Glassmeier
Ingo Richter

Institut für Geophysik und extraterrestrische Physik
Technische Universität Braunschweig
Mendelssohnstraße 3, 38106 Braunschweig
Germany

Anlage G2

R O S E T T A

FLIGHT REPORTS
of RPC–MAG

RO–IGEP–TR–0023

Issue: 3 Revision: 0

January 26, 2010

Report of the

Second Earth Swing By (ESB2)

Time period: November 07 - 20, 2007

Karl-Heinz Glassmeier
Ingo Richter

Institut für Geophysik und extraterrestrische Physik
Technische Universität Braunschweig
Mendelssohnstraße 3, 38106 Braunschweig
Germany

Anlage G3

R O S E T T A

FLIGHT REPORTS of RPC–MAG

RO–IGEP–TR–0029

Issue: 1 Revision: 0

March 30, 2010

Report of the

Third Earth Swing by (EAR3)

Time period: November 09 - 17, 2009

Ingo Richter
Karl-Heinz Glassmeier

Institut für Geophysik und extraterrestrische Physik
Technische Universität Braunschweig
Mendelssohnstraße 3, 38106 Braunschweig
Germany

Contents

1 Introduction

ROSETTA's third Earth Swing by (EAR3, ESB3) took place in the time interval November, 09 – 17, 2009. RPC-MAG was switched on from 2009-11-09T19:42:18 until 2009-11-17T17:15:00. The instrument performance was excellent.

This document gives a brief description of the executed activities and shows the obtained data. Housekeeping data (Temperature of the OB & IB sensor, Filter Stages A & B, Filter configuration register, Reference voltage, negative and positive 5V supply voltage, and the coarse HK sampled magnetic field data of the OB sensor) are presented as well as magnetic field science data of the OB and IB sensor in the activated modes. Magnetic field data are plotted in s/c coordinates and ECLIPJ2000 coordinates if not otherwise stated. They are calibrated according to the results of the ground calibration and the results of the inflight temperature model 006 using the actual flight data. Sensitivity, Misalignment, and Temperature effects are taken into account. The s/c residual field is not subtracted.

The data quality will be assessed and a comparison between OB and IB sensor will be presented in section 4.

Magnetic field data in GSE-coordinates are plotted in chapter 5. The detected magnetosphereic regions and plasma boundaries are presented in section 6.

The close Earth Swing by was a unique chance to check and improve the calibration of the instrument and to compare the measured field with a theoretical model (POMME) of the earth. These investigations will be presented in chapter 7.

Also the comparison of our magnetic field data with data measured by different spacecrafts (e.g WIND & ACE) can give information about the data quality. A comparison to the WIND & ACE data can be found in section 8.

The spectra of the magnetic field data measured by the OB sensor are plotted in section 9. As usual an influence of ROSETTAs reaction wheels (refer to section 10) can be seen in Burstmode.

A temperature profile for the whole Earth Swing by is shown in section 11.

The LANDER Magnetometer ROMAP was NOT switched on at this Swing by, so no data comparison between these two instruments can be made this time.

At the end of the Swing by a remaining Interference Test between MAG and LAP has been executed. This test took place from November 16, 15:00 until November 17, 17:15. The results can be found in in the Report RO-IGEP-TR0030.

2 The Swing by Geometry

This section gives an overview about the trajectory during the Swing by. ROSETTA approached through the night side within 5 days (November 9 until November 13), had its closest approach on November 13 at 07:45:30, and left through magnetopause and bow shock and the dayside. The closest approach distance to the Earth's surface was 2840 km.

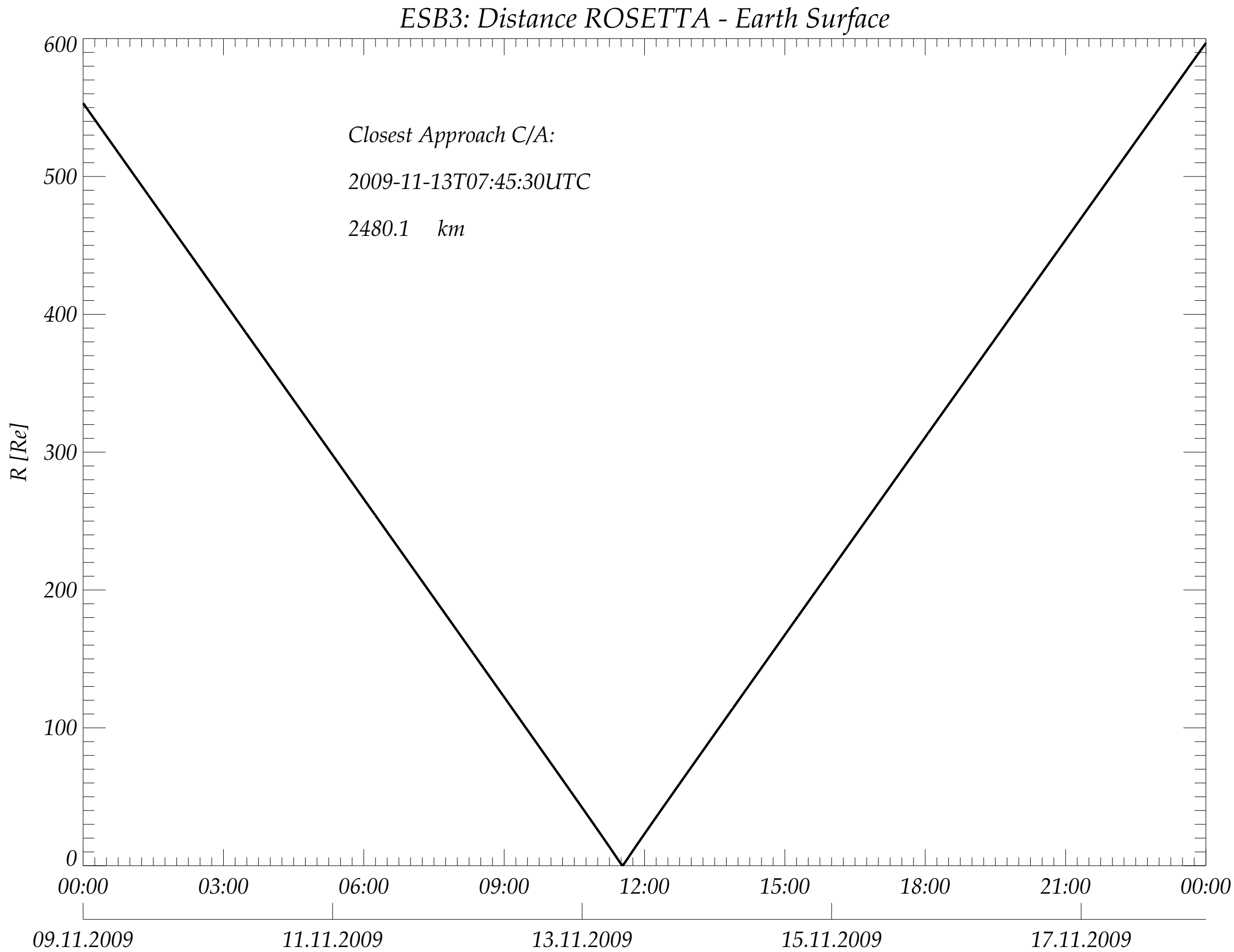

Figure 1: ROSETTA'S Distance to the EARTH'S Surface

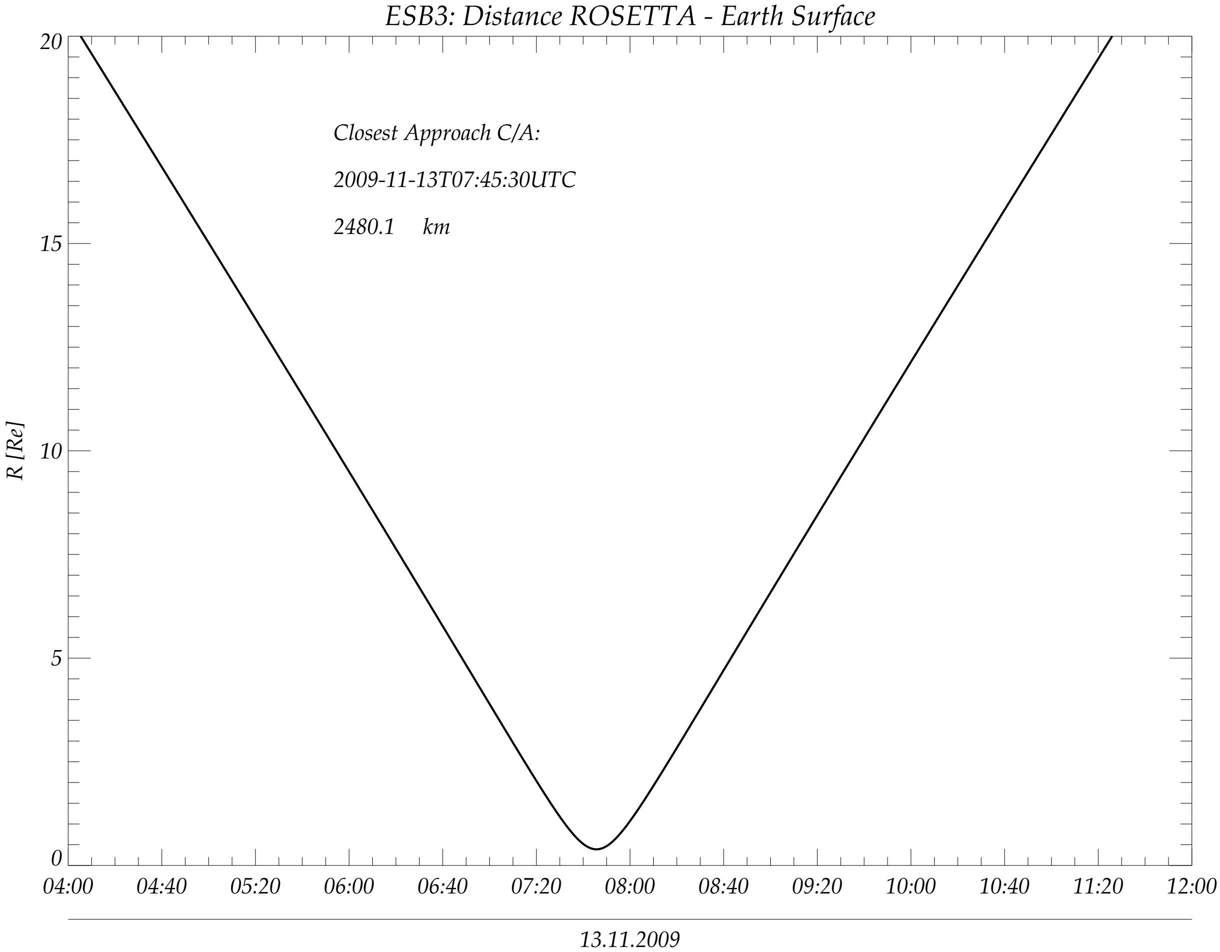

Figure 2: ROSETTA'S Distance to the EARTH'S Surface - zoomed view

The Figures 3 and 4 show the trajectory of ROSETTA in the plasma regime in the vicinity of the Earth. The used coordinate system is GSM (Geocentered Solar Magnetic), the black lines represent magnetic field lines derived from the Tsyganenko model, the dotted black line is the Bow Shock, the red line represents the magnetopause. The tick marks on ROSETTA's blue colored trajectory are two-hourly spaced. The magnetopause has been modelled using a dynamic pressure of 1.17nPa. This value has been derived from WIND and ACE measurements at that observing time. Refer to section 6 for a comparison with the measured data onboard ROSETTA.

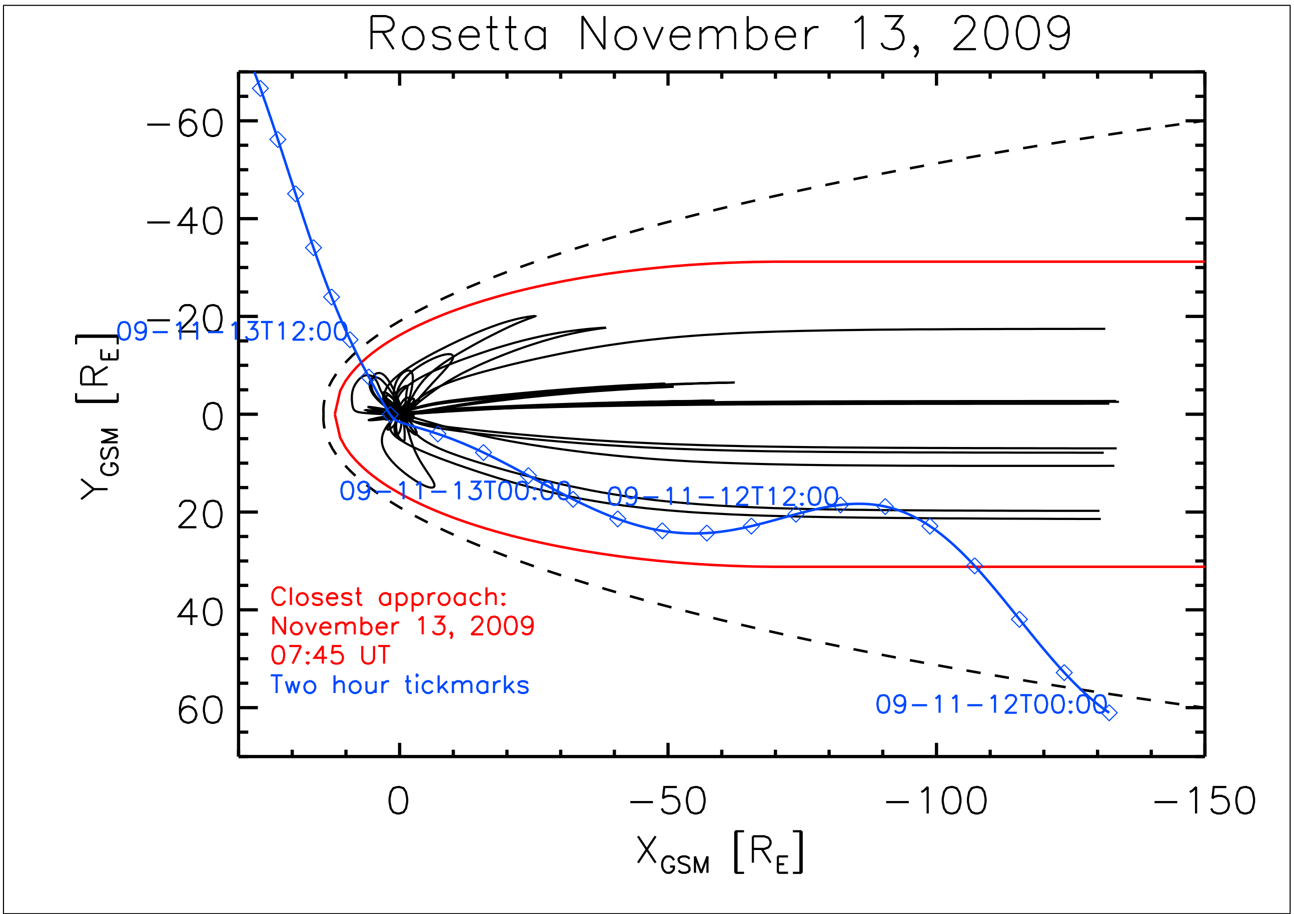

Figure 3: ROSETTA'S Swing by Trajectory in GSM coordinates: XY–Plane

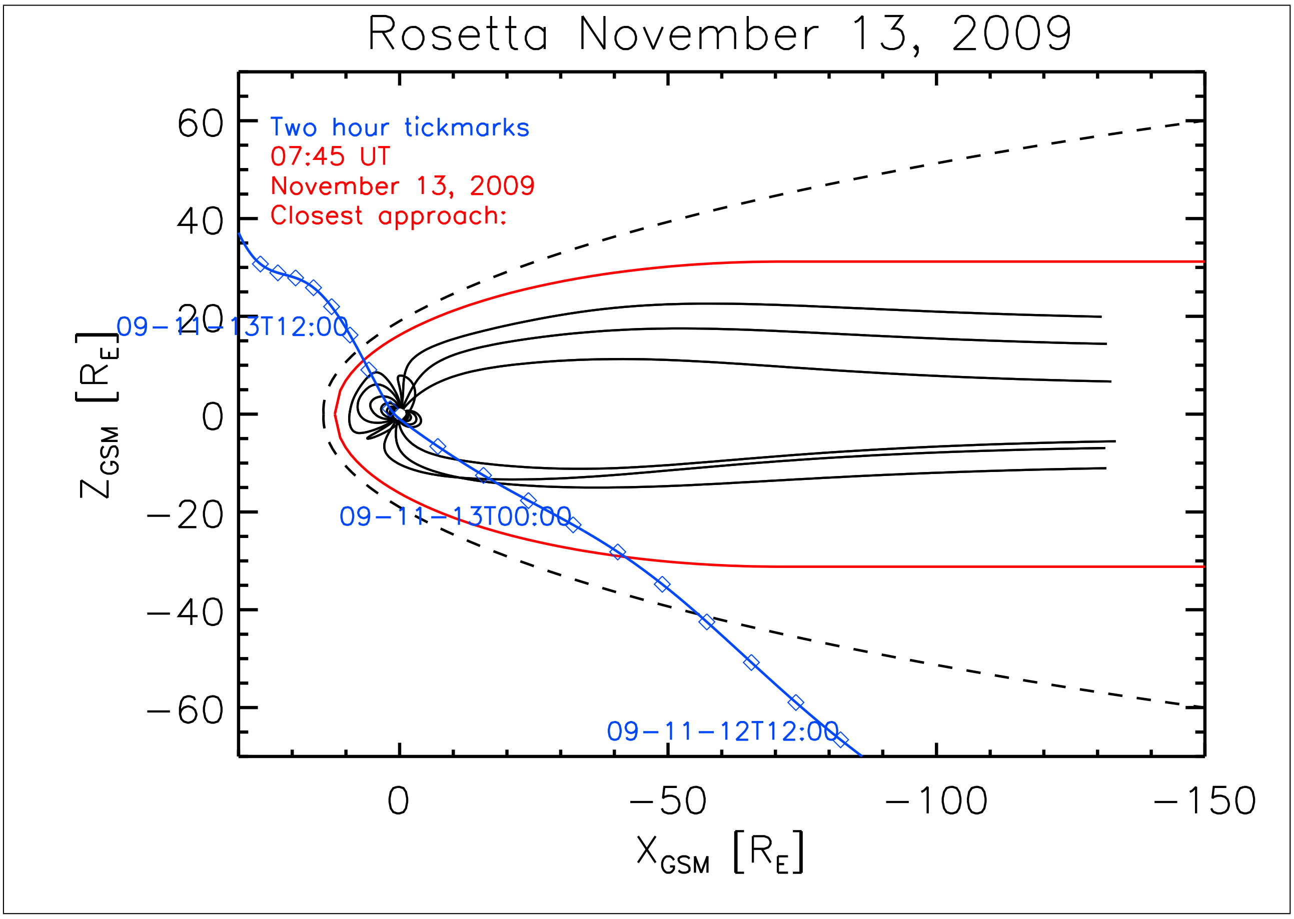

Figure 4: ROSETTA'S Swing by Trajectory in GSM coordinates: XZ–Plane

ROSETTA ESB3, November 13, 2009

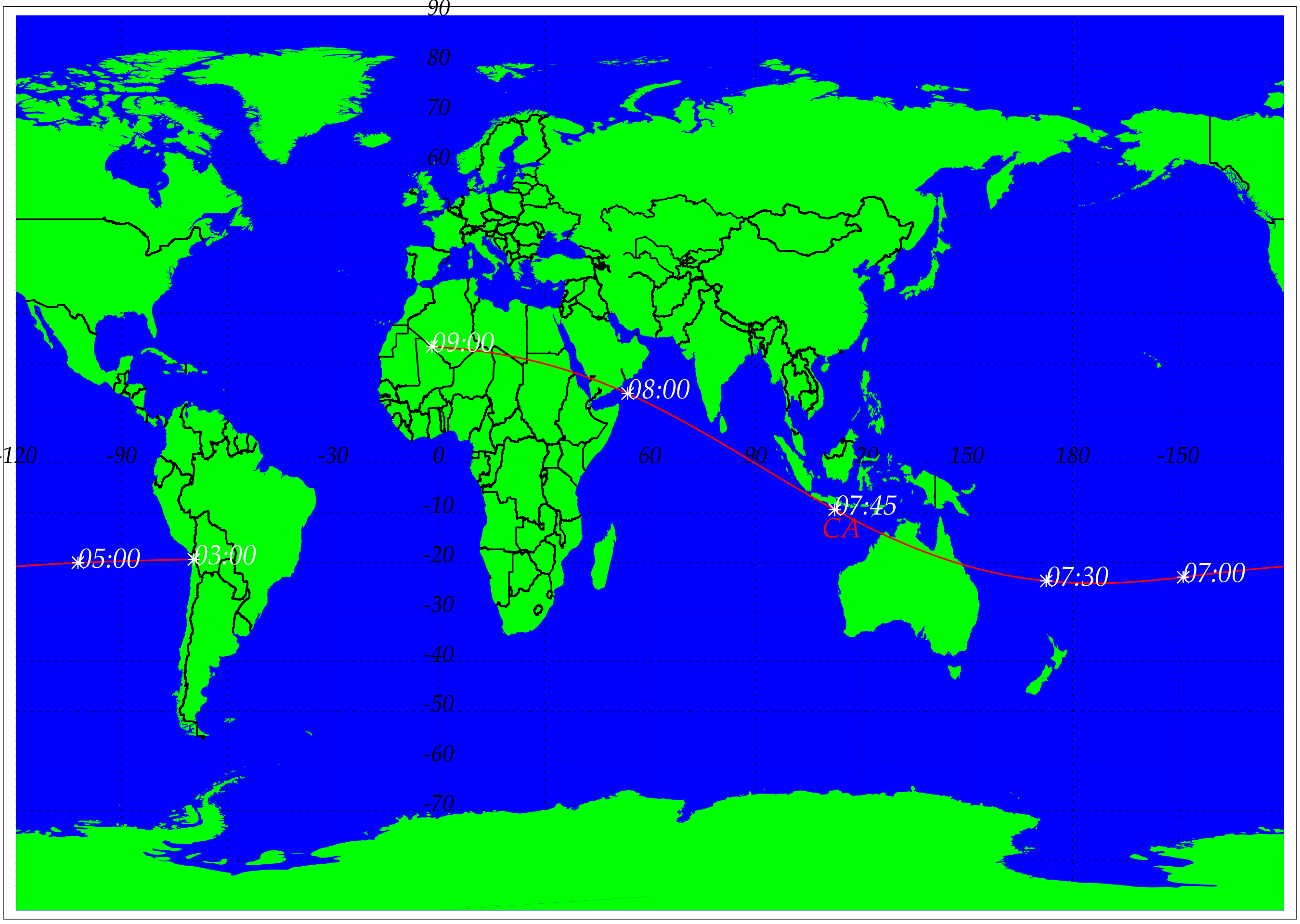

Figure 5: ROSETTA'S Ground Track during the Swing by

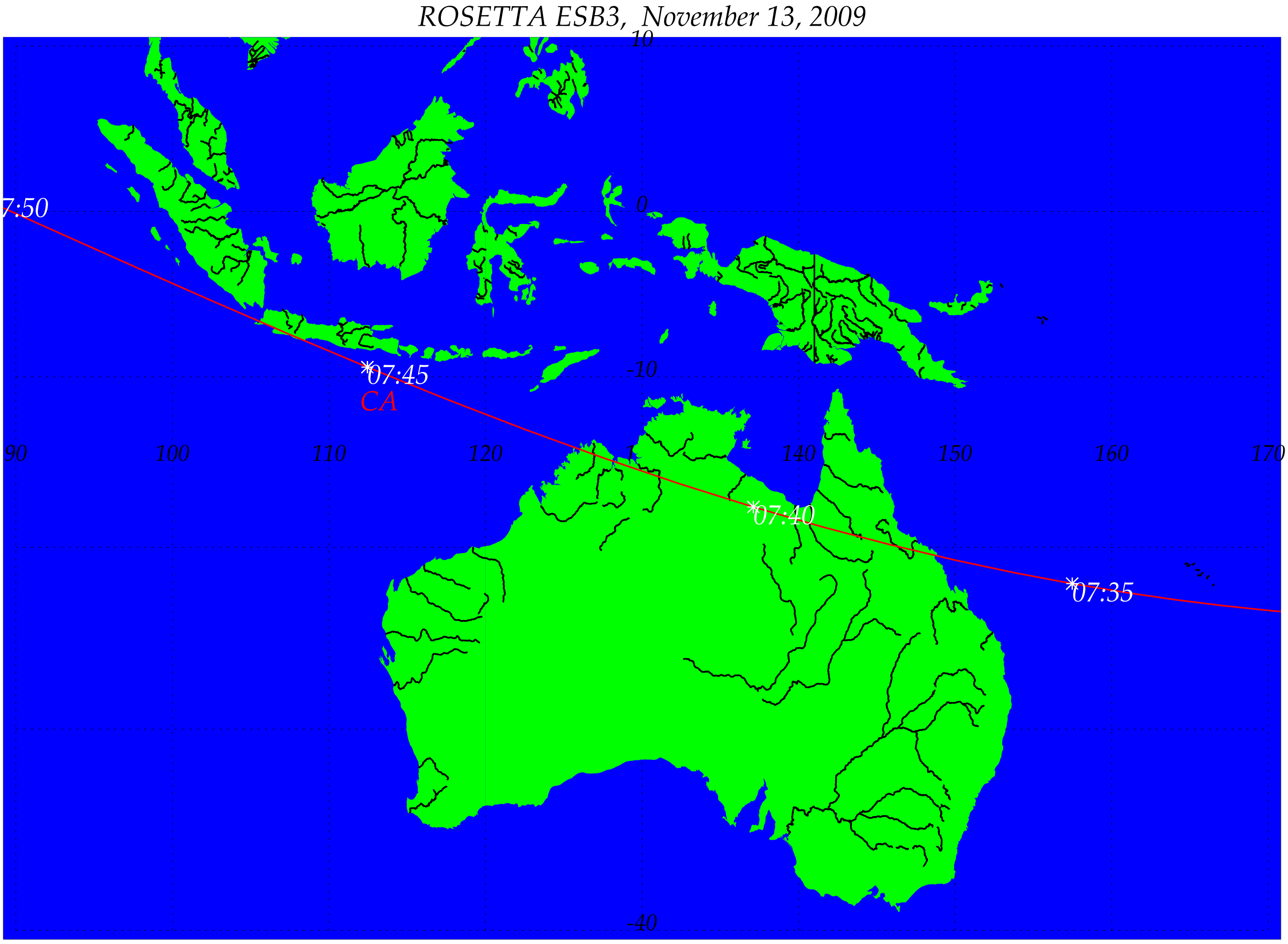

Figure 6: ROSETTA'S Ground Track during the Swing by (Zoomed)

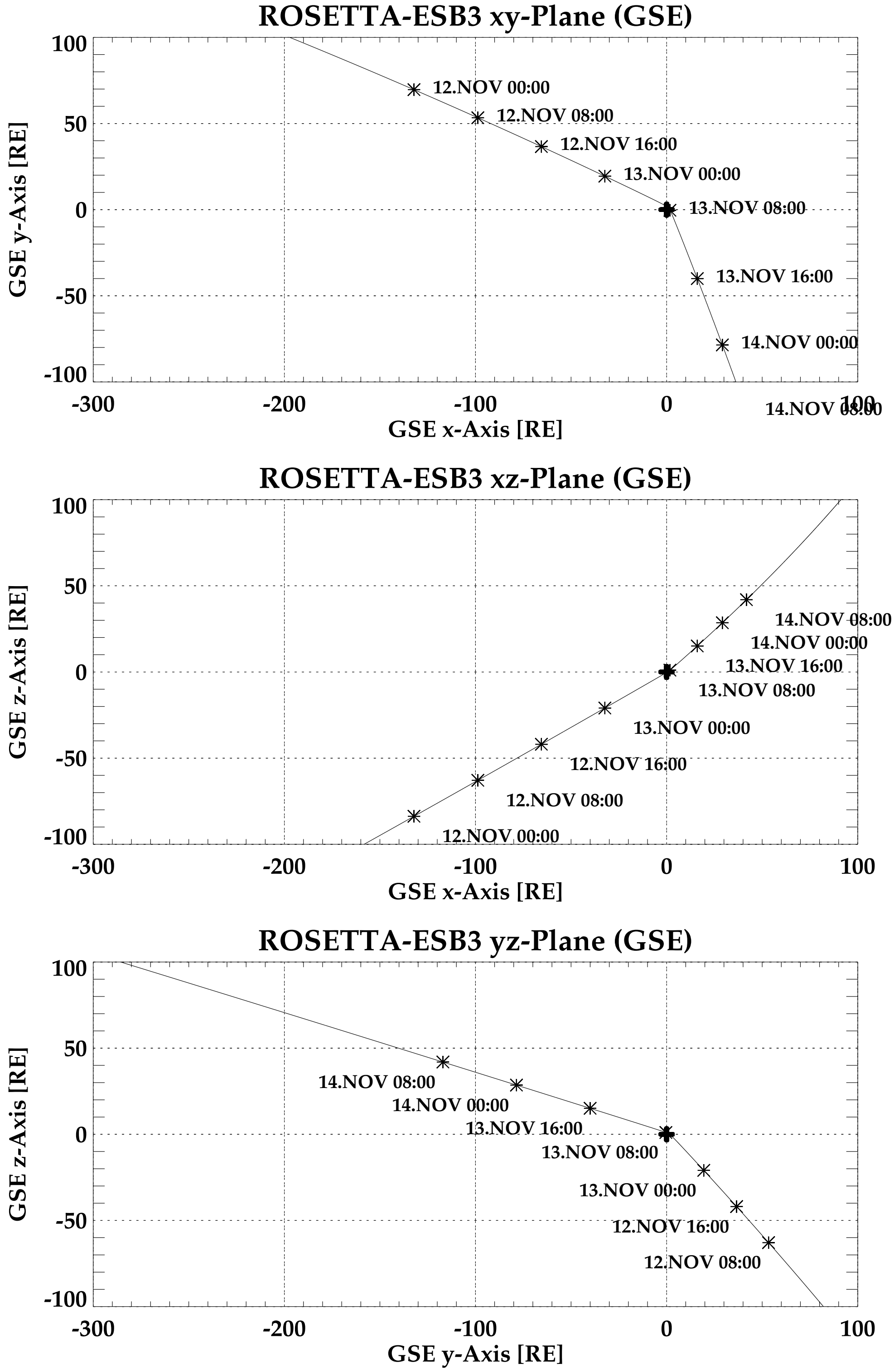

Figure 7: ROSETTA'S Trajectory in GSE coordiantes during the Swing by

Anlage H

R O S E T T A

FLIGHT REPORTS of RPC–MAG

RO–IGEP–TR–0022

Issue: 3 Revision: 0

January 25, 2010

Report of the

MARS Swing by (MSB)

Time period: February 23 - 27, 2007

Ingo Richter
Karl-Heinz Glassmeier

Institut für Geophysik und extraterrestrische Physik
Technische Universität Braunschweig
Mendelssohnstraße 3, 38106 Braunschweig
Germany

Contents

1 Introduction

ROSETTA's Mars Swing by (MSB) happened in the time period February 23 – 27, 2007. RPC-MAG was switched on in the time between 2007-02-23T00:00:54 and 2007-02-27T02:37:50. Around the closest Approach, however, all the orbiter payload was switched off due to power safety reasons. Therefore, there is a data gap for the time interval 2007-02-25T00:38:14 and 2007-02-25T02:35:42. The overall instrument performance was excellent. There were no problems.

This document gives a brief description of the executed activities and show the obtained data. Housekeeping data (Temperature of the OB & IB sensor, Filter Stages A & B, Filter configuration register, Reference voltage, negative and positive 5V supply voltage, and the coarse HK sampled magnetic field data of the OB sensor) are presented as well as magnetic field science data of the OB and IB sensor in the activated modes. Magnetic field data are plotted in s/c coordinates, ECLIPJ2000 coordinates and in Mars Solar Orbital (MSO) coordinates for the complete overview. The data are calibrated according to the results of the ground calibration and the results of the inflight temperature model 006 using the Mars flight data from February 2007. Sensitivity, Misalignment, and Temperature effects are taken into account. The s/c residual field is not subtracted. For details refer to section 5

The spectra of the magnetic field data measured by the OB sensor are plotted as well in section 7. The few measurements in BURST mode (SID3) in the hours around CA are disturbed by ROSETTAs reaction wheels (refer to section 6). This disturbance cam be eliminated d by our processing S/W.

At the end overview plots for the complete swing-by period are shown in ECLIPJ2000 and MSO coordinates.

2 The Swing-by Geometry

This section gives an overview about the trajectory during the MARS Swing-by. ROSETTA approached from the day side, had its closest approach on February 25 at 01:58, and left through tail region. The minimum distance to earth was 261 km.

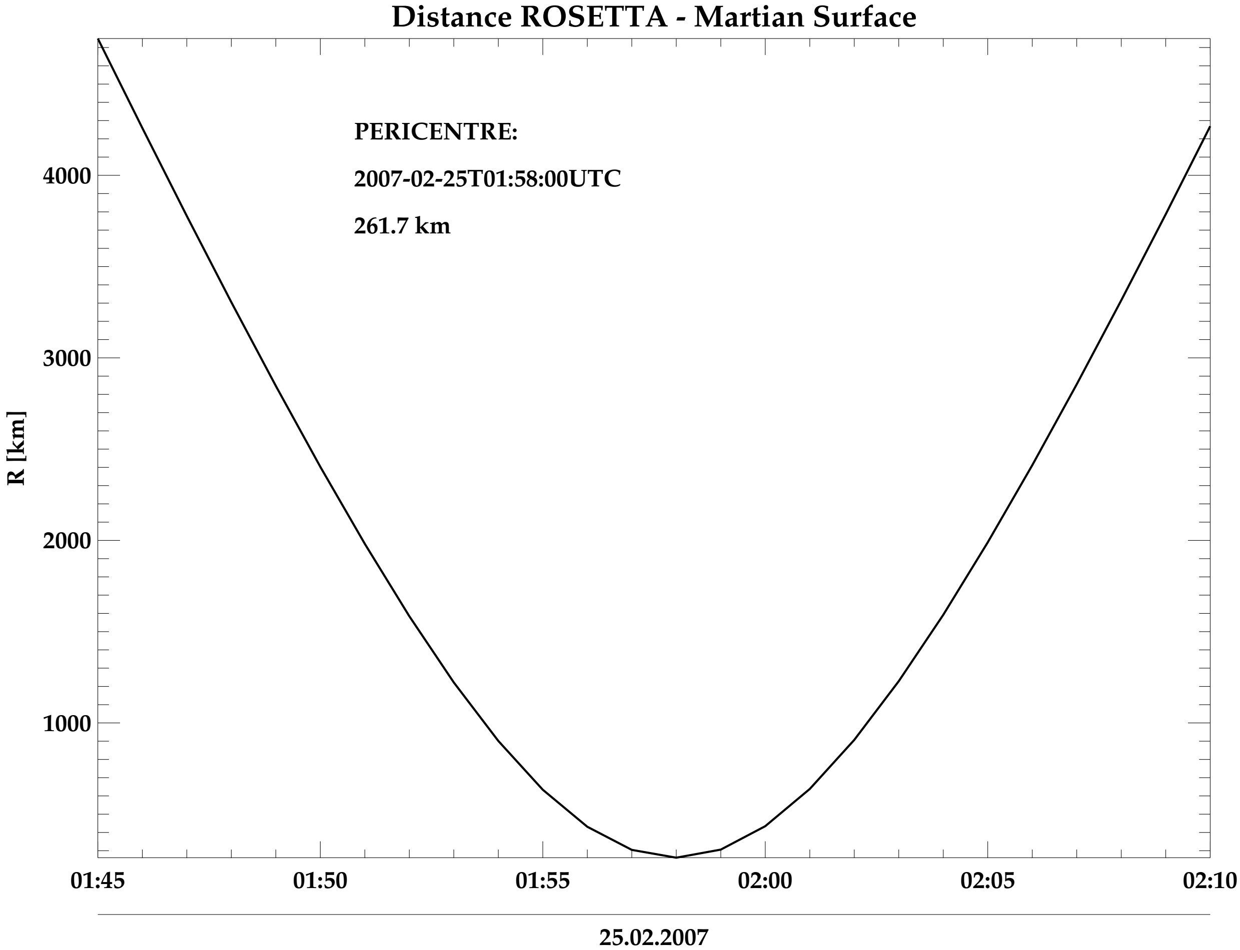

Figure 1: ROSETTA'S Distance to the Martian Surface

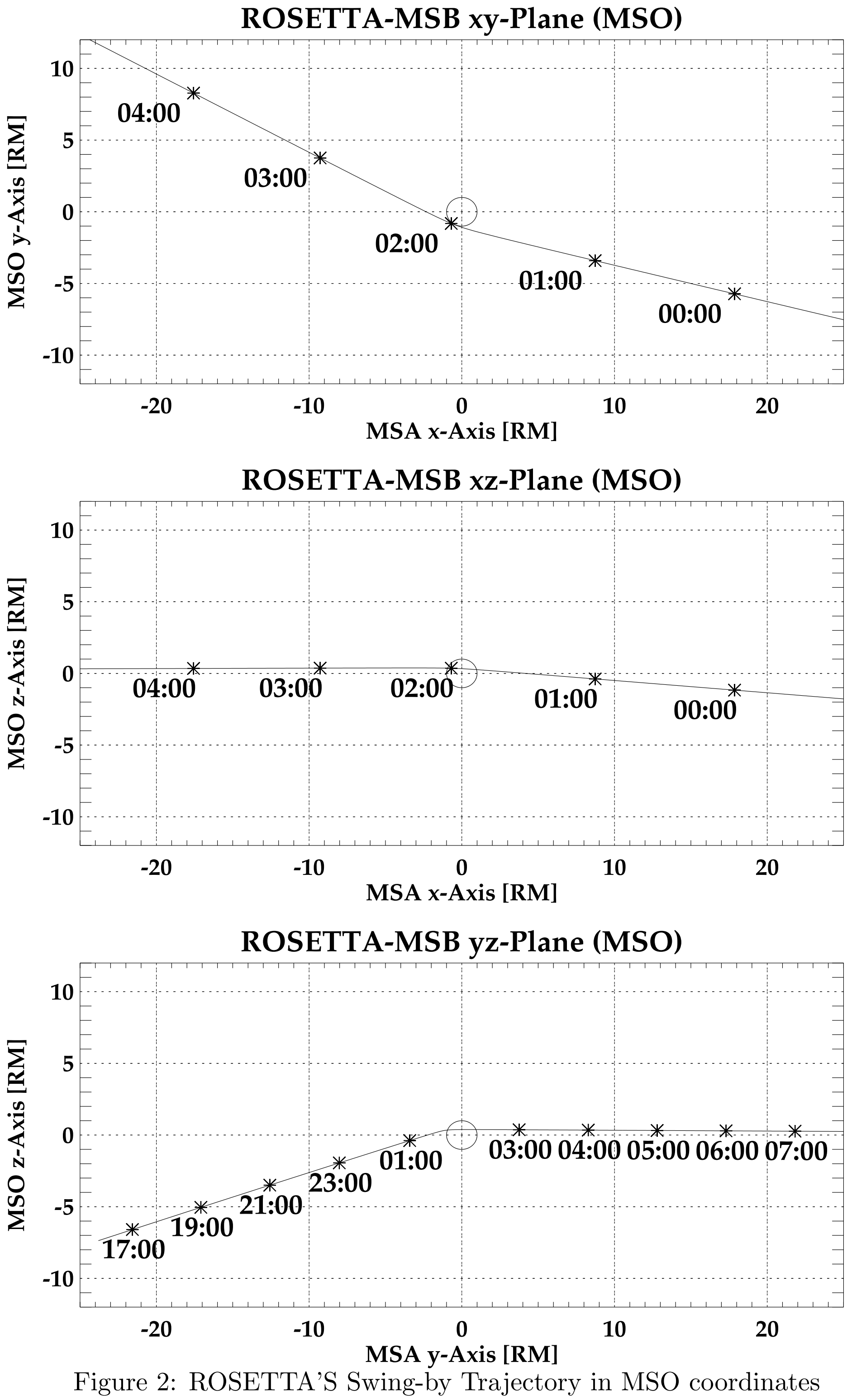

Figure 2: ROSETTA'S Swing-by Trajectory in MSO coordinates

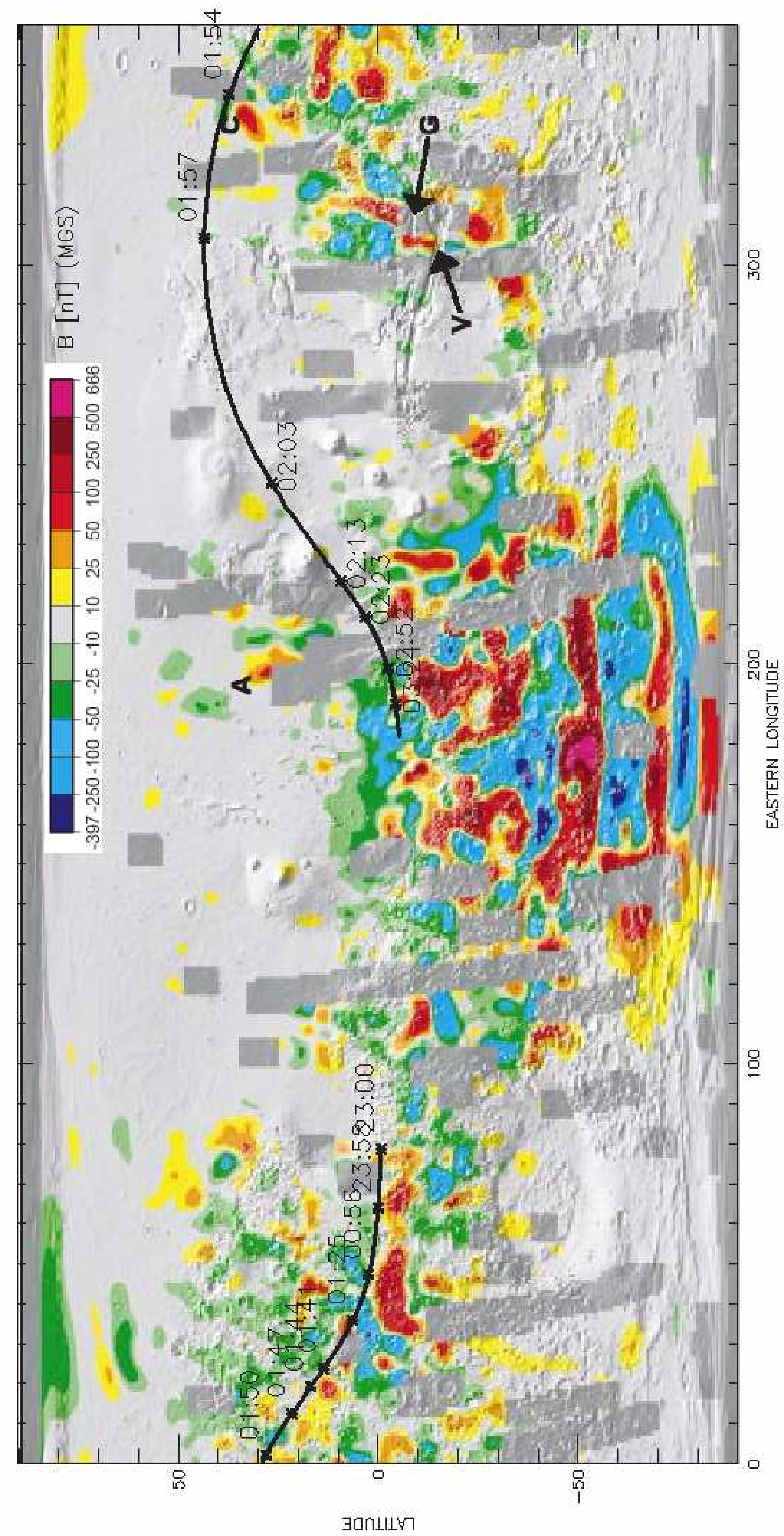

Figure 3: ROSETTA'S Swing-by ground track superimposed on MGS Magnetic Field Data

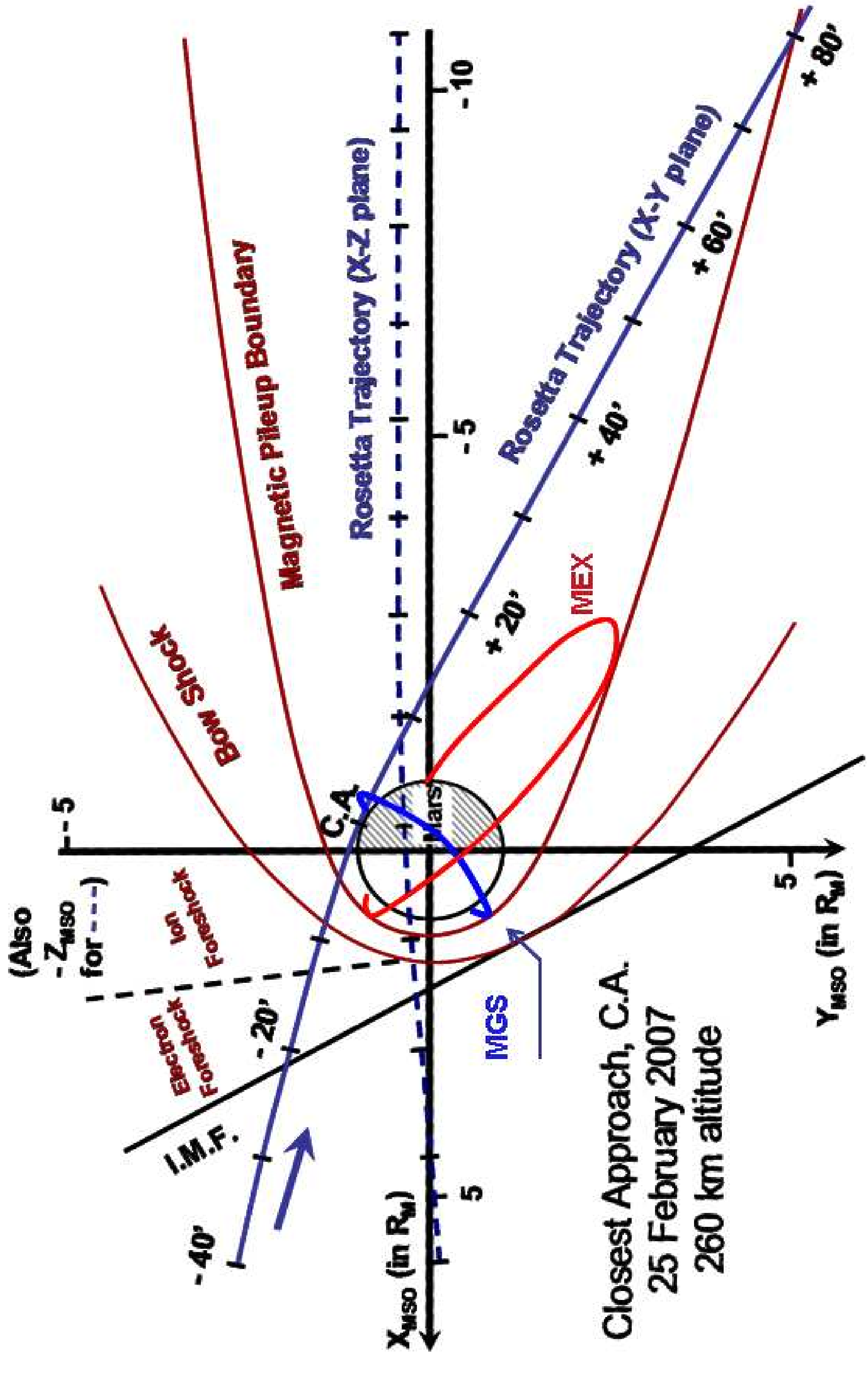

Figure 4: ROSETTA'S MARS Swingby Geometry (MSO)

Anlage I

Ann. Geophys., 27, 2383–2398, 2009
www.ann-geophys.net/27/2383/2009/

Annales Geophysicae

Rosetta swing-by at Mars – an analysis of the ROMAP measurements in comparison with results of 3-D multi-ion hybrid simulations and MEX/ASPERA-3 data

A. Boesswetter[1], U. Auster[2], I. Richter[2], M. Fränz[4], B. Langlais[5], S. McKenna-Lawlor[6], S. Simon[1], U. Motschmann[1,3], K. H. Glassmeier[2], N. J. T. Edberg[7], and R Lundin[8]

[1]Institute for Theoretical Physics, TU Braunschweig, Germany
[2]Institute for Geophysics and Extraterrestrial Physics, TU Braunschweig, Germany
[3]DLR, Institute of Planetary Research, Berlin, Germany
[4]Max Planck Institute for Solar System Research, Katlenburg-Lindau, Germany
[5]CNRS, Laboratoire de Planétologie et Géodynamique, Nantes Atlantique Universités, Nantes, France
[6]Space Technology Ltd., National University of Ireland, Maynooth, County Kildare, Ireland
[7]Department of Physics & Astronomy, University of Leicester, Leicester, UK
[8]Swedish Institute of Space Physics, Kiruna, Sweden

Received: 15 May 2008 – Revised: 7 May 2009 – Accepted: 25 May 2009 – Published: 8 June 2009

Abstract. The Rosetta spacecraft flew by Mars at a distance of 260 km on 25 February 2007 during a gravity assist manoeuvre. During the closest approach (CA) the lander magnetometer ROMAP was switched on. The dataset taken during this swingby provides insight into the plasma environment around Mars: in addition to a pronounced bow shock crossing Rosetta recorded the signature of the pile up region of draped magnetic field. Also the Rosetta measurements showed signatures of crustal magnetic field anomalies which can be verified by results of a crustal magnetic field model. In order to understand the measured field morphology, multi-ion hybrid simulations were performed. Some of the input parameters for the simulations were obtained from Mars Express (MEX) data which were contemporaneously collected during the Rosetta swingby. These simulations reproduces ROMAP magnetic field measurements and show that the interplanetary magnetic field pointed northward during the encounter. A spectral analysis shows upstream waves ahead of the bow shock and indicates the presence of the magnetic pile-up boundary (MPB). The multi-ion model reproduces the ion fluxes measured by MEX/ASPERA-3 and is in agreement with the measurements to within one order of magnitude.

Correspondence to: A. Boesswetter
(a.boesswetter@tu-bs.de)

Keywords. Interplanetary physics (Planetary bow shocks) – Magnetospheric physics (Plasma waves and instabilities) – Space plasma physics (Kinetic and MHD theory)

1 Introduction

On 2 March 2004 ESA scientists celebrated the successful launch of the Rosetta spacecraft aboard an Ariane 5 launcher from Kourou in French Guyana to comet 67P/Churyumov-Gerasimenko (Glassmeier et al., 2007a). Before the spacecraft reaches its target, a series of swing-by manoeuvres will be accomplished. After the first Earth swingby in March 2005 Rosetta successfully performed a Mars swingby in February 2007. Within the framework of this paper, we focus on plasma and magnetic field observations during the latter swingby. First the data will be discussed and secondly the output from a three-dimensional, multi-species hybrid model will provide a reference to support our analyses. The hybrid approach treats the electrons of the plasma as a fluid, while the ions are represented by individual particles. Thus, this approximation is capable of incorporating effects like non-Maxwellian velocity distributions and differences between the flow patterns of the involved ion species. These phenomena become of importance when the overall size of the interaction region is comparable to the gyroradii of the ions, as is the case at Mars.

Published by Copernicus Publications on behalf of the European Geosciences Union.

Anlage J

Anlage K

R O S E T T A

FLIGHT REPORTS
of RPC–MAG

RO–IGEP–TR–0025

Issue: 3 Revision: 0

January 26, 2010

Report of the

STEINS Flyby

Time period: September 01 - 10, 2008

Karl-Heinz Glassmeier
Ingo Richter

Institut für Geophysik und extraterrestrische Physik
Technische Universität Braunschweig
Mendelssohnstraße 3, 38106 Braunschweig
Germany

Contents

1 Introduction

ROSETTA's Flyby at asteroid 2867 STEINS happened on September 05, 2008. RPC-MAG was switched on in the time between 2008-09-01T00:10:00 and 2008-09-10T06:01:00. The Closest Approach (CA) took place at 2008-09-05T18:38:19.3 (Onboard UTC). The instrument performance was flawlessly. There were no problems from the instrument side.

This document gives a brief description of the executed activities and show the obtained data. Housekeeping data (Temperature of the OB & IB sensor, Filter Stages A & B, Filter configuration register, Reference voltage, negative and positive 5V supply voltage, and the coarse HK sampled magnetic field data of the OB sensor) are presented as well as magnetic field science data of the OB and IB sensor in the activated modes. Magnetic field data are plotted in s/c coordinates and ECLIPJ2000 coordinates if not otherwise stated. They are calibrated according to the results of the ground calibration and the results of the inflight temperature model 006 using the actual flight data. Sensitivity, Misalignment, and Temperature effects are taken into account. The s/c residual field is not subtracted.

The spectra of the magnetic field data measured by the OB sensor are plotted in section 5. As usual an influence of ROSETTAs reaction wheels (refer to section 6) can be seen in Burstmode.

From time to time there are also horizontal lines in the dynamic spectrum to be seen. These lines represent constant frequencies and are caused by the LAP instrument. This behavior was investigated and proofed during the PC10 campaign in November 2010. See RO-IGEP-TR0030 for further details.

The data quality and a comparison between OB and IB sensor is presented in section 4.

The activation of the LANDER was combined with the test of some heaters associated to the MUPUS experiment. Unfortunately this caused magnetic disturbances which are also discussed in section 4.

The Rotation Angles of the Solar Arrays and the High Gain Antenna have been plotted in section 7 for the assessment of their influence to the magnetic field data.

A temperature profile for the whole Fly–By is shown in section 8.

2 The Fly–By Geometry

This section gives an overview about the trajectory during the Fly–By.

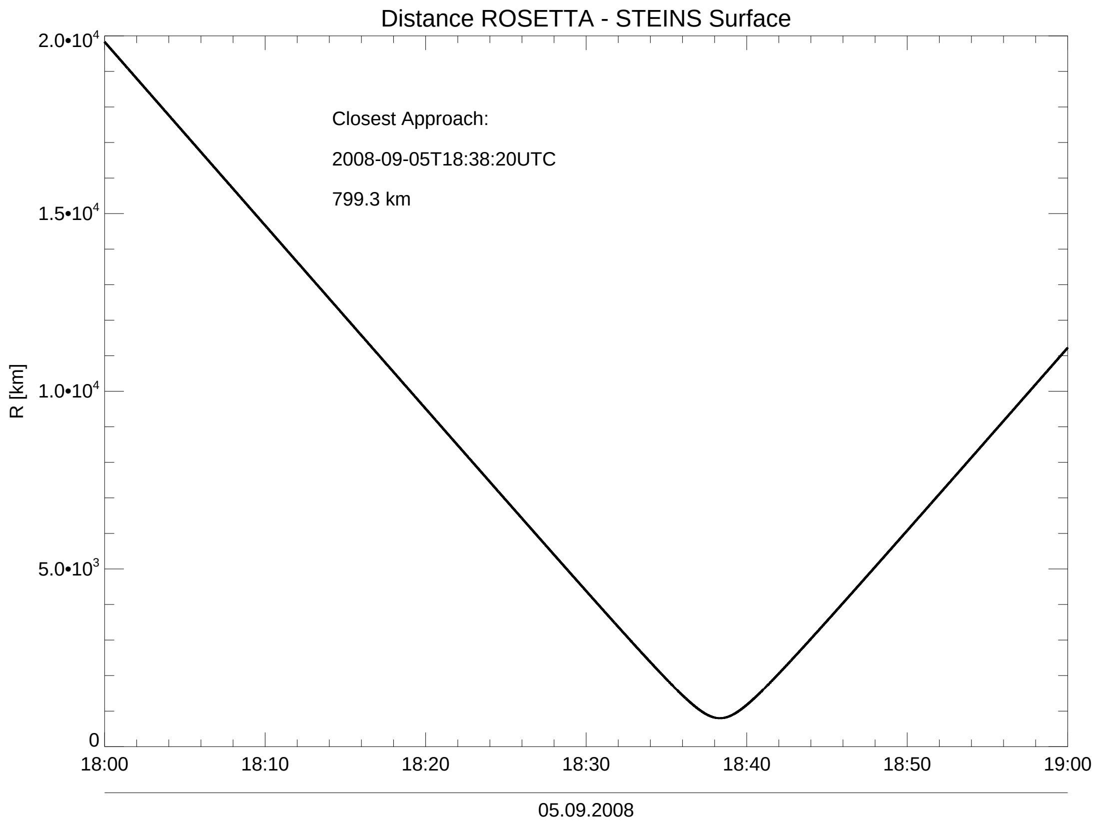

Figure 1: ROSETTA'S Distance to the STEINS Surface

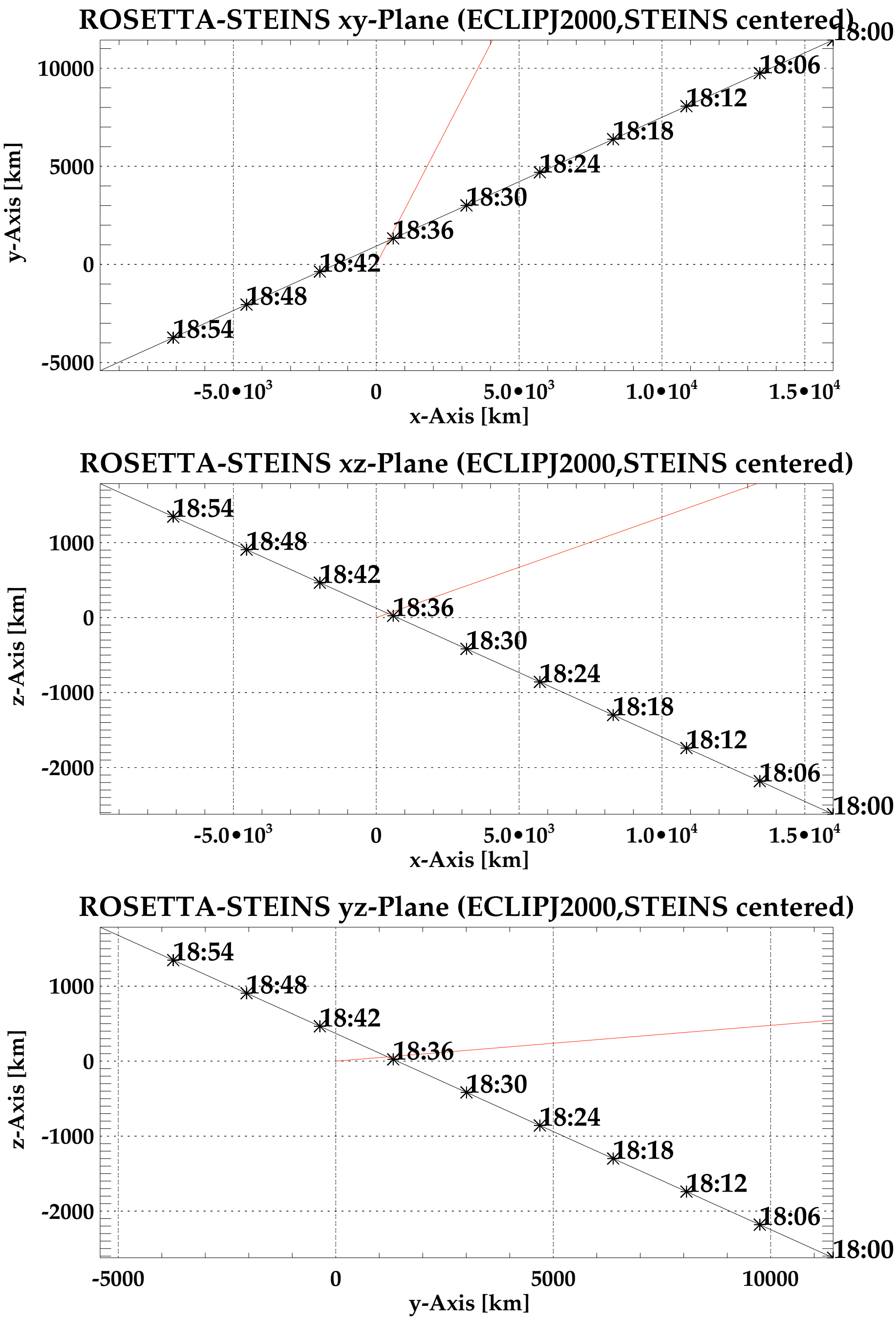

Figure 2: ROSETTA'S Fly-By Trajectory in ECLIPJ2000 coordinates. Red Line: SUN Direction

Anlage L

Magnetic Field Investigations During ROSETTA's 2867 Šteins Flyby

H.U. Auster [a,*], I. Richter [a], K.H. Glassmeier [a,b], G. Berghofer [e], C.M. Carr [c], U. Motschmann [d,f]

[a] *Institut für Geophysik und extraterrestrische Physik, Technische Universität Braunschweig, Germany*

[b] *Max Planck Institute for Solar System Research, Katlenburg-Lindau, Germany*

[c] *Imperial College, London, United Kingdom*

[d] *Institut für Theoretische Physik, Technische Universität Braunschweig, Germany*

[e] *Space Research Institute, Austrian Academy of Sciences, Graz, Austria*

[f] *Institut für Planetenforschung, Deutsches Zentrum für Luft- und Raumfahrt, Berlin, Germany*

Abstract

During the 2867 Šteins flyby of the ROSETTA spacecraft **on September 5, 2008** magnetic field measurements have been made with both the RPC orbiter magnetometer and the ROMAP lander magnetometer. These combined magnetic field measurements allow a detailed examination of any magnetic signatures caused either directly by the asteroid or indirectly by Šteins' different modes of interaction with the solar wind. Comparing measurements with simulation results show that Šteins does not posses a significant remanent magnetization. The magnetization is estimated at less than 10^{-3}Am^2/kg. This is significantly different from results at 9969 Braille and 951 Gaspra.

Key words: asteroids, Šteins, ROSETTA, magnetic field, remanent magnetization

* Institut für Geophysik und extraterrestrische Physik, Technische Universität Braunschweig, Mendelssohnstr. 3, D-38106 Braunschweig, Germany

Email address: `uli.auster@tu-bs.de` (H.U. Auster).

1 Asteroids and their magnetic properties

Meteorites are unique materials of the solar system in their ability to provide information on the magnetic properties of their parent asteroidal bodies. Magnetic measurements reveal natural remanent magnetization between about $10^{-3}\mathrm{Am}^2/\mathrm{kg}$ for basaltic achondrites, $10^{-1}\mathrm{Am}^2/\mathrm{kg}$ for chondrites, and $1\mathrm{Am}^2/\mathrm{kg}$ for stony-irons [e.g. Cisowski, 1987, 1991, Collinson, 1994, Terho et al., 1996]. However, meteorites were subject to heavy alteration, brecciation, shock, or metamorphic events. This may have altered their magnetic properties, and any conclusion about the magnetization of their parent body is difficult [e.g. Weiss et al., 2008]. Therefore, more direct magnetic field measurements at asteroids are important and necessary to understand their physical properties and how they were formed in our early solar system.

The first direct measurement of an asteroidal magnetic field was reported by Richter et al. [2001] using magnetic field observations made during the encounter of the Deep Space 1 spacecraft with asteroid 9969 Braille on July 29, 1999 at an approximate distance of 28 kilometer. The magnetic moment estimated from these flyby observations amounts to $2.1 \cdot 10^{11}\mathrm{Am}^2$, corresponding to a specific magnetic moment of $2.8 \cdot 10^{-2}\mathrm{Am}^2/\mathrm{kg}$.

The first magnetic field measurements at the surface of an asteroid were conducted with the magnetometer experiment onboard the NEAR spacecraft which landed on the surface of asteroid 433 Eros on 12 February 2001 [Acuña et al., 2002]. These measurements reveal a global scale magnetization of less than $1.9 \cdot 10^{-6}\mathrm{Am}^2/\mathrm{kg}$.

Already in 1991 the Galileo spacecraft passed by asteroid 951 Gaspra at a distance of 1600 km. Magnetic field measurements made onboard Galileo reveal a change in direction of the interplanetary magnetic field near closest approach at Gaspra [Kivelson et al., 1993]. The magnetic field rotated toward Gaspra about a minute before closest approach and back to its original direction afterwards. Kivelson et al. [1993] have interpreted this rotation as evidence of magnetic field draping around Gaspra as a magnetospheric obstacle. As Gaspra is a highly irregular object with principal diameters of 18.2, 10.5, and 8.9 km and a mean radius of 6.1 km [Thomas et al., 1994] this obstacle has to be much greater than these scales, which indicates the presence of a magnetospheric type interaction region caused by an asteroidal magnetic field. Kivelson et al. [1993] estimated a magnetic dipole moment for Gaspra of about $6 \cdot 10^{12}$ to $2 \cdot 10^{14}\mathrm{Am}^2$. Estimating its mass at about $2 \cdot 10^{15}$ kg gives one a specific magnetic moment of $(0.3 - 10) \cdot 10^{-2}\mathrm{Am}^2/\mathrm{kg}$. Such a magnetization is in the range observed in meteorites, especially those with an ordinary chondrite composition [e.g. Hood and Sonett, 1994]. It also conforms to the measurements reported from the Deep Space 1 flyby at 9969 Braille [Richter et al., 2001].

The question emerging is how bodies like Gaspra and Braille can acquire such a significant magnetization. Aggregation of permanently magnetized iron dust can serve as building material for larger permanently magnetized celestial objects [e.g. Nübold and Glassmeier, 2000]. Small bodies such as chondrules and perhaps some meteorites may acquire a thermoremanent magnetization from the solar nebula magnetic field as they cool [e.g. Uehara and Nakamura, 2006]. But it is unlikely that the spin axis of larger bodies could have remained fixed relative to the nebula magnetic field for a sufficient time for the whole body becoming uniformly magnetized. Thus, the question arises whether Braille's or Gaspra's magnetization was acquired while it was still part of a parent body with a magnetic field generated by a dynamo process.

The magnetic Reynolds number $\mathrm{R_m} = \mu_0 \, \sigma \, u \, L$, where L is a typical length scale of the system operating a dynamo, for example, the radius of an asteroid parent body, σ the electrical conductivity, and u the speed of the convecting material, determines whether or not a system can support dynamo action to generate a magnetic field. For a dynamo to be able to operate, this magnetic Reynolds number should be large. Thus, a dynamo can only operate in a large, electrically conducting core in the presence of heavy convection. Therefore, asteroids and their parent bodies are often regarded as objects not being able to support a dynamo because of their small spatial scale.

However, recent paleomagnetic studies of some of the oldest known pristine basaltic meteorites, the angrites, indicate that their magnetization could well be due to an early dynamo in a rapidly formed metallic core [Weiss et al., 2008]. Nimmo [2009] discusses the conditions under which such a small body can operate a dynamo. In depth studies of the magnetic properties therefore are a most useful and important tool to understand the formation and dynamics of asteroids and their parent bodies.

The recent flyby of the ROSETTA spacecraft [Glassmeier et al., 2007a] at asteroid 2867 Šteins provided an excellent possibility to further study the magnetic properties of an asteroid by spacecraft measurements. 2867 Šteins is an E-type asteroid with a possible enstatite achondrite surface. The heavily brecciated enstatite achondrite meteorites, the Aubrites, are believed to have E-type asteroids as their parent bodies [e.g. Weissman et al., 2008]. Magnetic properties of aubrites have been studied by e.g. Brecher et al. [1979] and Pesonen et al. [1993] and indicate a very low specific magnetic moment, less than $10^{-3}\mathrm{Am^2/kg}$. For a few aubrites such as the ALHA 78113, Norton County, Cumberland Falls, and Bishopville meteorites we have performed our own, additional measurements on the magnetic properties these meteorites. The magnetization ranges between $10^{-5}\mathrm{Am^2/kg}$ and $10^{-3}\mathrm{Am^2/kg}$. The question is whether such a low remnant magnetization can be detected during a spacecraft flyby.

2 Magnetic Interaction Scenarios

The optimum observational situation to measure any asteroidal magnetic field is, of course, a direct measurement at the surface of the body. This, however, is a very demanding observational goal. The alternative is a flyby allowing a direct or indirect observational determination of the asteroidal magnetic field. Direct observations during a flyby as reported by Richter et al. [2001] are only possible if the flyby distance is very close, at least of the order of the spatial scale of the asteroid.

Indirect determination of the magnetic field requires knowledge about the type of interaction of the asteroid and the magnetized solar wind plasma. Determination of the type of interaction using spacecraft observations allows, at least qualitatively, to classify the asteroidal magnetic field. Greenstadt [1971] discusses in detail the conditions under which a magnetized object can generate a magnetosphere as it exists around planet Earth: the magnetopause distance needs to be larger than the spatial scale R_A of the object, that is the magnetic pressure should be larger than the dynamic pressure of the solar wind. If M is the magnetic dipole moment, $\mathrm{v_{SW}}$ the solar wind speed at large distance to the object, and ρ_{SW} its mass density, the magnetopause distance R_{MP} is given as

$$R_{MP} = \sqrt[6]{\frac{2\mu_0 M^2}{\rho_{SW} v_{SW}^2}}. \tag{1}$$

With $M = m \cdot \rho_A \cdot V_A$, where m is the specific magnetic moment, and ρ_A and $V_A = 4\ \pi/3\ R_A^3$ are the mass density of the asteroid and its volume, respectively, we have

$$(\frac{R_{MP}}{R_A})^6 \approx 4 \cdot 10^{-5} \frac{\rho_A^2}{\rho_{SW} v_{SW}^2} m^2, \tag{2}$$

or, with $\rho_A = 3 \cdot 10^3 \mathrm{kg/m^3}$, $\rho_{SW} = 1.3 \cdot 10^{-20} \mathrm{kg/m^3}$, and $\mathrm{v_{SW}} = 400$ km/s,

$$\frac{R_{MP}}{R_A} \approx 75 \cdot m^{1/3}. \tag{3}$$

Thus, only a body with a specific magnetization of about $1\mathrm{Am^2/kg}$ or larger would give rise to a typical magnetospheric type interaction region. Magnetospheric type interaction regions have been studied using numerical simulations by e.g. Wang and Kivelson [1996], Blanco-Cano et al. [2003], or Simon et al. [2006]. When an asteroid's global magnetic moment is sufficiently strong, an interaction region with magnetospheric structure develops. Downstream of the asteroid a region exists from which the solar wind is excluded. Furthermore, the interaction region is surrounded by a boundary layer which indicates the presence of a bow shock. The interplanetary magnetic field clearly exhibits draping features around the obstacle and is characterized by strong modifications of the plasma density (see Fig. 1). The detection of a clear draping signature of the interplanetary magnetic field around an asteroid is therefore an indirect measurement of an asteroidal magnetization of the order 1 $\mathrm{Am}^2/\mathrm{kg}$ and larger.

For lower asteroidal magnetic fields, that is a specific magnetization of $0.5 \cdot 10^{-3}$ to $0.5 \cdot 10^{1} \mathrm{Am}^2/\mathrm{kg}$ Greenstadt [1971] already suggested a different type of interaction with strong whistler wave activity to be expected. Numerical simulations by [e.g. Baumgärtel et al., 1997] confirm this prediction (Fig. 2). The interaction in this sub-magnetospheric situation is characterized by low-frequency plasma waves which are phase-standing in the asteroid frame of reference. The characteristics of these waves are controlled by the direction of the interplanetary magnetic field relative to the solar wind flow direction and by the orientation of the asteroids magnetic moment [Baumgärtel et al., 1997]. Simulations indicate that a magnetic moment of least $10^{12}\mathrm{Am}^2$ is required to produce observable perturbations in the interplanetary magnetic field at a distance of approximately 1000 km from the asteroid.

For values of the specific magnetization of less than about $10^{-4}\mathrm{Am}^2/\mathrm{kg}$ an asteroid is not at all an obstacle to the solar wind plasma, hardly modifying the interplanetary magnetic field in any significant manner.

These considerations show that three major different types of interaction can be identified (Fig. 3): a magnetospheric, a whistler-wave, and a non-magnetic type of interaction. Any flyby can be classified according to this classification and allows at least a qualitative determination of the magnetic properties of the asteroid visited. A magnetospheric type interaction is only expected for a specific magnetic moment larger than 10 $\mathrm{Am}^2/\mathrm{kg}$, a magnetization comparable to industrial permanent magnets. For chondrites and stony iron meteorite parent bodies a whistler-wave type interaction is expected. For objects like Eros a non-magnetic interaction is likely.

Based on this classification magnetic field observations made at 2867 Šteins during the ROSETTA flyby were used to estimate the magnetic properties of this asteroid.

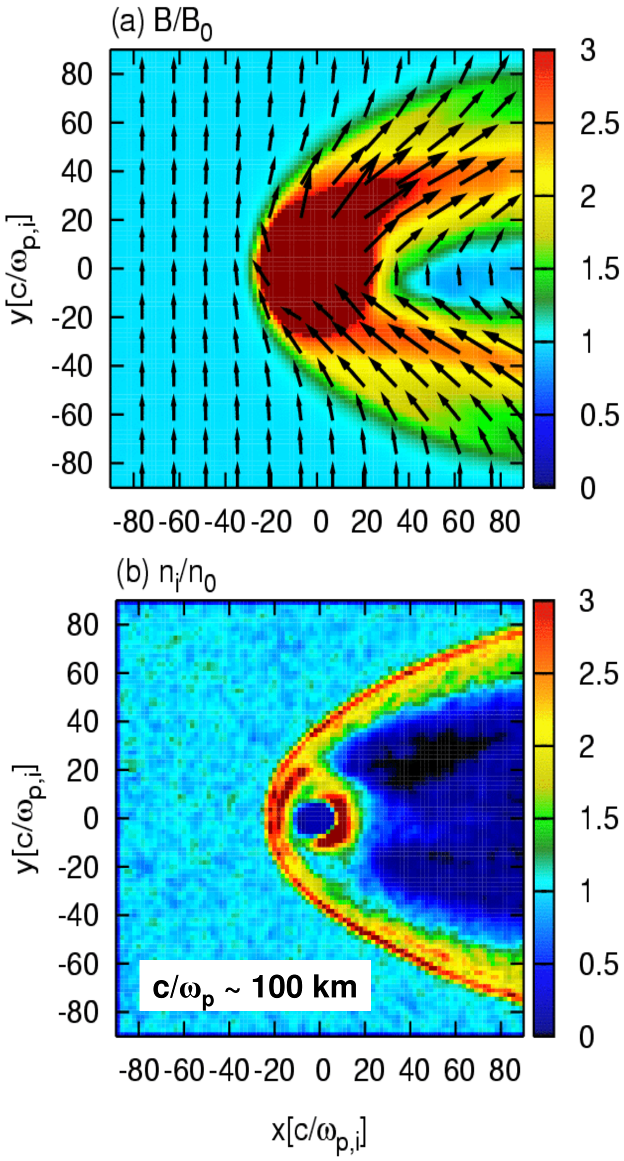

Fig. 1. Numerical simulation of the magnetic field and plasma mass density perturbations in the interaction region of the solar wind with a strongly magnetized asteroid (after Simon et al. [2006]). The upper panel displays the magnetic field draping caused by the interaction, the lower plasma density structures. The axes are scaled by the proton inertial length c/ω_{pi}.

3 ROSETTA Magnetic Field Observations

The ROSETTA spacecraft [Glassmeier et al., 2007a] encountered asteroid 2867 Šteins on September 5, 2008. Closest approach occurred at 18:38 UTC at a distance of 799 km. The flyby distance is displayed

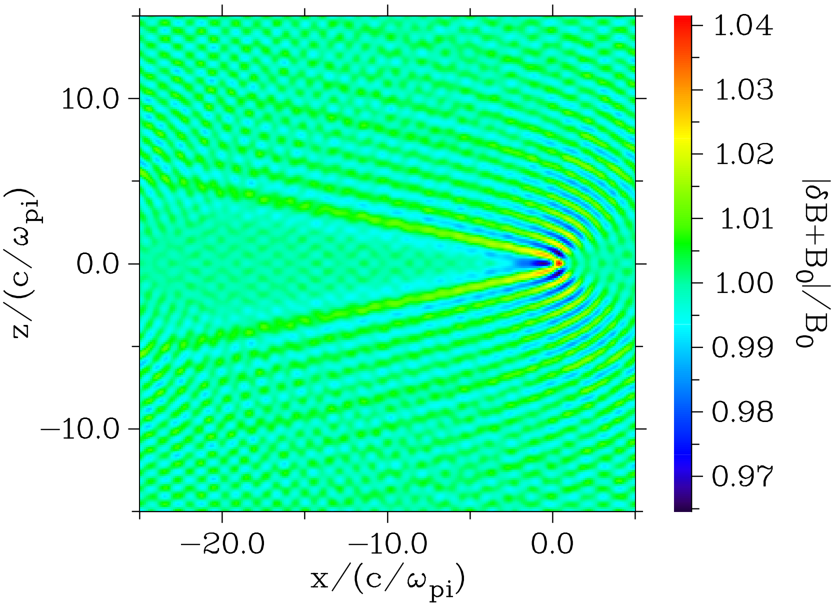

Fig. 2. Stationary response of a solar wind flow with Alfvén Mach number $M_A = 8$ and a plasma $\beta = 1$ to a weakly magnetized asteroid, idealized as a line dipole, with the magnetic moment, the solar wind flow, and the interplanetary magnetic field being co-aligned. The spatial variation of the normalized magnetic field amplitude $\delta B + B_0/B_0$ is shown and the axes are scaled by the proton inertial length c/ω_{pi} (after Baumgärtel et al. [1997]).

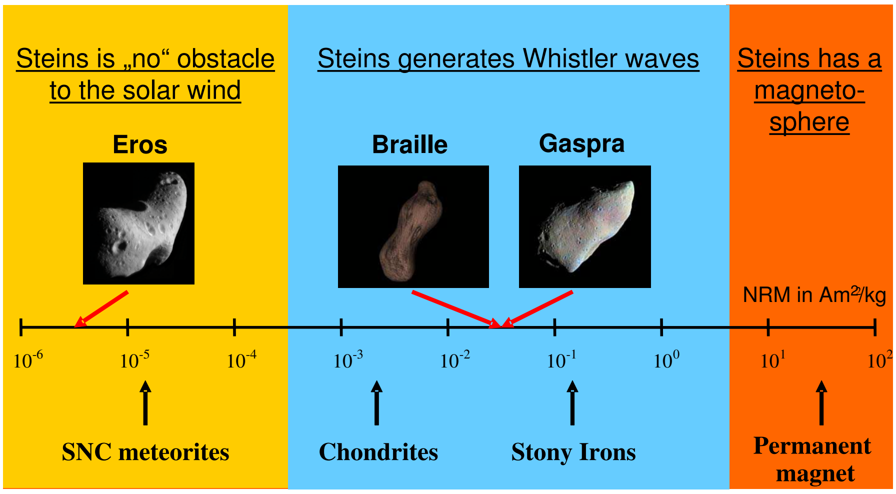

Fig. 3. The three qualitatively different interaction regions between an asteroid and the magnetized solar wind plasma as anticipated in advance of the flyby of ROSETTA at 2867 Šteins: the non-magnetic interaction regime (yellow), the whistler-wave regime (blue), and the magnetospheric regime (orange). The Eros magnetization is in the range of the shergottite, nakhlite, and chassigny (SNC) class of meteorites; the natural remanent magnetization (NRM) causing a magnetosphere is comparable to permanent magnets.

in Fig. 4; for further details of the flyby geometry reference is made to Accomazzo et al. [2010]. During the encounter the fluxgate magnetometer experiments onboard the ROSETTA orbiter [Glassmeier et al., 2007b] and the Rosetta Lander PHILAE [Auster et al., 2007] were switched-on and fully operational. This provided for a unique opportunity to study any magnetic field of asteroid 2867 Šteins and the type of interaction of 2867 Šteins with the solar wind plasma.

The orbiter magnetometer system RPC-MAG measures the magnetic field vector by its two sensors, the inboard and the outboard sensor with a digital resolution of 30 pT, a 20-bit measurement range, and a maximum sample rate of 20 Hz; at Šteins data were taken at 0.03 and 1 Hz, respectively. For the present analysis only data from the outboard sensor were used. Further instrument details are described in Glassmeier et al. [2007b] and Carr et al. [2007]. Although the magnetometer sensors are mounted on a short boom, they are still influenced by magnetic fields generated by the spacecraft itself. Known disturbances are caused by the reaction wheels controlling the spacecraft attitude and by spacecraft heaters

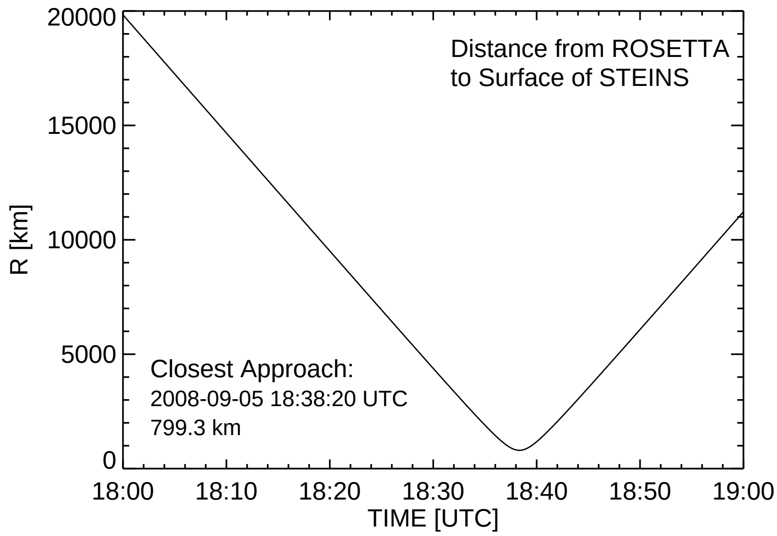

Fig. 4. **ROSETTA - Šteins flyby distance.**

which are operated by electric currents and therefore generate magnetic fields. The reaction wheel disturbance [Glassmeier et al., 2007b] can be purged using a special filter algorithm in the frequency domain with knowledge of the four varying reaction wheel frequencies.

Furthermore the signals of the magnetic field sensors are temperature dependent, so especially a spacecraft flip which brings the normally shadowed sensors into bright sunlight generates a strong temperature increase which needs to be taken into account for data processing. At Šteins the temperature changed from $-125°$ C to $-75°$ C. Additionally, the raw data have to be rotated into a suitable coordinate system to be scientifically accessible. The data processing pipeline applied to the data taken at Šteins thus contains the following steps for every measured field vector: apply the results from the magnetometer ground calibration with temperature dependent sensitivity and misalignment matrices, take the temperature dependent sensor offset into account by usage of a cubic polynomial modelling of the temperature behavior, rotate the resulting magnetometer vector from instrument to spacecraft-coordinates, use a jump detection to remove deterministic field jumps caused by currents flowing on the lander PHILAE, rotate the magnetic field vector from spacecraft coordinates to time and space dependent celestial coordinates, taking into account the actual s/c attitude (SPICE kernels provide the information needed here), and finally, time average the data to a suitable mean.

A similar procedure is applied to the ROMAP data. The PHILAE magnetometer is located in the vicinity of the cables carrying the disturbing currents. Thus, the disturbing amplitude is much higher at ROMAP and can be used as a "disturbance-proxy" for the correction of the RPC-MAG signal. Elimination of disturbances seen on RPC-MAG can easily be done by subtraction a suitable fraction of the ROMAP magnetic signal from the RPC-MAG data.

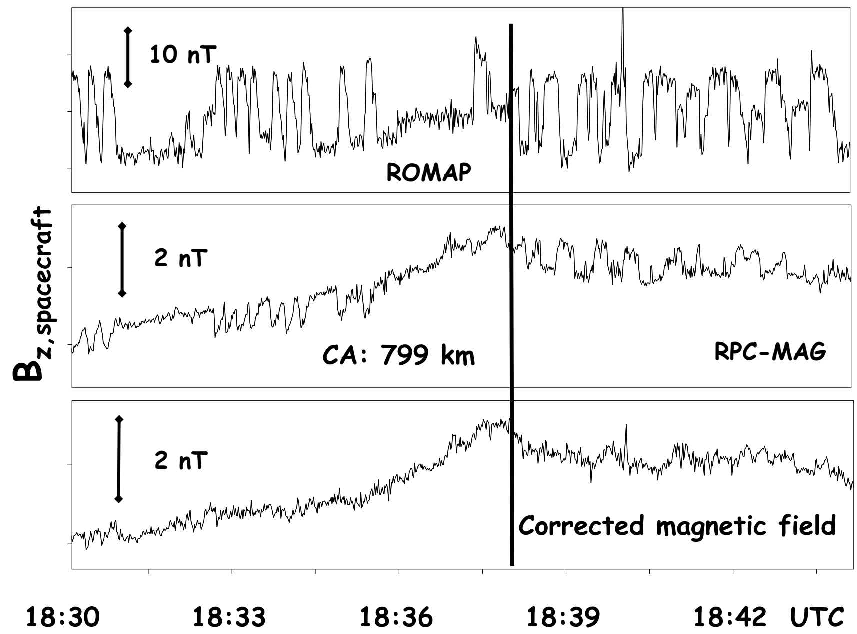

Fig. 5. Uncorrected magnetic field observations from the ROMAP and RPC magnetometers (top two traces) and the B_z of the corrected field as seen during the time period around closest approach.

To illustrate the processing procedure uncorrected magnetic field measurements from the ROMAP and RPC magnetometers are displayed in Fig. 5 together with the processed magnetic field signal after applying all the above mentioned steps to the raw magnetic field time series. Two major features can be derived from the result. First, even if the data are highly influenced by secondary effects it is possible to achieve scientifically meaningful data and second, the parallel operation of two spatially separated magnetometers allows to distinguish between "disturbance" and "science" signal. For the first time both magnetometers operate at a sequence in which most of the scientific instruments are active. The level of magnetic disturbances was representative for those we can expect during the main science phase of the mission. We showed that spacecraft generated interference fields can be detected and removed by using both magnetometers. A common operation during the comet approach phase is highly recommended in order to study the magnetic characteristics of the spacecraft and orbiter instruments in further detail. After release of PHILAE this knowledge has to be applied to remove related instrument signatures.

An overview of the magnetic field measurements during the flyby is shown in Fig. 6. The data are represented in the ECLIPJ2000 frame, an ecliptic inertial reference frame related to the Equinox of Epoch J2000. This reference frame is defined as follows: the X axis is pointing from the Sun to the Vernal Equinox,

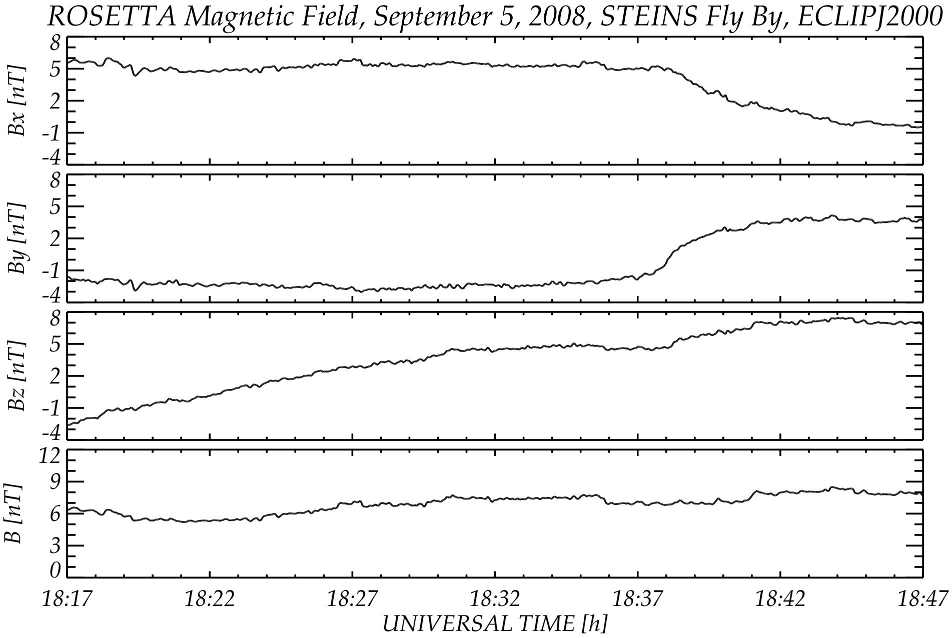

Fig. 6. Magnetic field observations made during the ROSETTA Šteins flyby on September 5, 2008. Closest approach occurred at 18:38 UT. The ECLIPJ2000 frame of reference is used. The data shown are derived from using measurements form both magnetometer systems. **The offset error is about ±1 nT, the relative error about ±0.1 nT.**

which is the intersection of the mean orbital plane of the Earth (ecliptic) and the mean equatorial plane at the epoch J2000, the Z axis is perpendicular to the X axis and pointing "up", perpendicular to the ecliptic, and the Y axis is lying in the ecliptic plane and completes the frame to be a right handed coordinate system.

The interplanetary magnetic field during the flyby interval is rather quiet. The field magnitude is almost constant while the B_Z component exhibits a continuous variation from -4 nT to about 8 nT. Only around closest approach the B_X and B_Y components show a clear rotation of the magnetic field vector in the ecliptic plane, a signature very common in the solar wind. We do not interpret this rotation as being caused by the asteroid as the rotation is not at all localized and the magnitude is unchanged.

4 Summary and Conclusions

We conclude from the observations displayed in Fig. 6 that any asteroid associated magnetic field disturbance in the 2867 Šteins solar wind interaction is less than 1 nT. This implies that the specific magnetization of Šteins is less than 10^{-3}Am^2/kg.

Magnetic properties of aubrites have been studied by e.g. Brecher et al. [1979] and Pesonen et al. [1993]. Additional measurements were conducted for this study. In each case the results indicate a very low specific magnetic moment between 10^{-5}Am^2/kg and 10^{-3}Am^2/kg. These magnetization values are well in accord with our qualitative determination of the magnetization of asteroid 2867 Šteins. This not only confirms our actual measurements but also indicates the importance of in-situ measurements at asteroids.

Future studies on asteroidal magnetic fields are necessary. The ESA mission Marco Polo is an excellent opportunity to realize such a measurement. Furthermore, theoretical and numerical studies on early dynamo action in solar system planetesimals is important further work.

5 Acknowledgements

We are especially indebted to Lucy McFadden, University of Maryland, and Ansgar Greshake, Naturkundemuseum Berlin, who made available aubrites whose magnetic properties we analyzed for this study. Financial support of the work of HUA, KHG, and IR at the Technical University of Braunschweig by the German Ministerium für Wirtschaft und Technologie and the Deutsches Zentrum für Luft- und Raumfahrt under grant 50 QP 0402 is acknowledged.

References

Accomazzo, A., Wirth, K. R., Lodiot, S., Kppers, M., and Schwehm, G. (2010) The flyby of asteroid Šteins. *Planet. Space Sci.*, in press.

Acuña, M. H., Anderson, B. J., Russell, C. T., Wasilewski, P., Kletetshka, G., Zanetti, L., and Omidi, N. (2002). NEAR Magnetic Field Observations at 433 Eros: First Measurements from the Surface of an Asteroid. *Icarus*, 155:220–228.

Auster, H. U., Apathy, I., Berghofer, G., Remizov, A., Roll, R., Fornacon, K. H., Glassmeier, K. H., Haerendel, G., Hejja, I., Kührt, E., Magnes, W., Moehlmann, D., Motschmann, U., Richter, I., Rosenbauer, H., Russell, C. T., Rustenbach, J., Sauer, K., Schwingenschuh, K., Szemerey, I., and Waesch, R. (2007). ROMAP: Rosetta Magnetometer and Plasma Monitor. *Space Sci. Rev.*, 128:221–240.

Baumgärtel, K., Sauer, K., Story, T. R., and McKenzie, J. F. (1997). Solar Wind Response to a Magnetized Asteroid: Linear Theory. *Icarus*, 129:94–105.

Blanco-Cano, X., Omidi, N., and Russell, C. T. (2003). Hybrid simulations of solar wind interaction with magnetized asteroids: Comparison with Galileo observations near Gaspra and Ida. *J. Geophys. Res.*, 108:1216–1224.

Brecher, A., Fuhrman, M., and Stein, J. (1979). The Magnetic Effects of Brecciation and Shock in Meteorites: III. The Achondrites. *Moon and Planets*, 20:265–279.

Carr, C., Cupido, E., Lee, C. G. Y., Balogh, A., Beek, T., Burch, J. L., Dunford, C. N., Eriksson, A. I., Gill, R., Glassmeier, K. H., Goldstein, R., Lagoutte, D., Lundin, R., Lundin, K., Lybekk, B., Michau, J. L., Musmann, G., Nilsson, H., Pollock, C., Richter, I., and Trotignon, J. G. (2007). RPC: The Rosetta Plasma Consortium. *Space Sci. Rev.*, 128:629–647.

Cisowski, S. M. (1987). Magnetism of meteorites. In Jacobs, J., editor, *Geomagnetism, Vol. 2*, volume 2, pages 525–556. Academic Press, London.

Cisowski, S. M. (1991). Remanent magnetic properties of unbrecciated eucrites. *Earth Planet. Sci. Lett.*, 107:173–181.

Collinson, D. W. (1994). The Magnetism of Meteorites and Early Solar System Magnetic Fields. *Roy. Soc. London Phil. Trans., Series A*, 349:197–207.

Glassmeier, K.-H., Boehnhardt, H., Koschny, D., Kührt, E., and Richter, I. (2007a). The Rosetta Mission: Flying Towards the Origin of the Solar System. *Space Sci. Rev.*, 128:1–4.

Glassmeier, K.-H., Richter, I., Diedrich, A., Musmann, G., Auster, U., Motschmann, U., Balogh, A., Carr, C., Cupido, E., Coates, A., Rother, M., Schwingenschuh, K., Szegö, K., and Tsurutani, B. (2007b). RPC-MAG The Fluxgate Magnetometer in the ROSETTA Plasma Consortium. *Space Sci. Rev.*, 128:649–670.

Greenstadt, E. W. (1971). Conditions for Magnetic Interaction of Asteroids with the Solar Wind. *Icarus*, 14:374–381.

Hood, L. L. and Sonett, C. P. (1994). Galileo Magnetic Field Signature: No Evidence That Gaspra is Differentiated. In *Lunar and Planetary Institute Science Conference Abstracts*, volume 25 of *Lunar and Planetary Inst. Technical Report*, pages 561–562.

Kivelson, M. G., Bargatze, L. F., Khurana, K. K., Southwood, D. J., Walker, R. J., and Coleman, P. J. (1993). Magnetic field signatures near Galileo's closest approach to Gaspra. *Science*, 261:331–334.

Nimmo, F. (2009). Energetics of asteroid dynamos and the role of compositional convection. *Geophys. Res. Lett.*, 36:10201–10205.

Nübold, H. and Glassmeier, K.-H. (2000). Accretional Remanence of Magnetized Dust in the Solar Nebula. *Icarus*, 144:149–159.

Pesonen, L. J., Terho, M., and Kukkonen, I. T. (1993). Physical properties of 368 meteorites: Implications for meteorite magnetism and planetary geophysics. *Antarctic Meteorite Research*, 6:401–417.

Richter, I., Brinza, D. E., Cassel, M., Glassmeier, K.-H., Kuhnke, F., Musmann, G., Othmer, C., Schwingenschuh, K., and Tsurutani, B. T. (2001). First direct magnetic field measurements of an asteroidal magnetic field: DS1 at Braille. *Geophys. Res. Lett.*, 28:1913–1916.

Simon, S., Bagdonat, T., Motschmann, U., and Glassmeier, K.-H. (2006). Plasma environment of magnetized asteroids: a 3-D hybrid simulation study. *Annales Geophysicae*, 24:407–414.

Terho, M., Pesonen, L. J., and Kukkonen, I. T. (1996). Magnetic properties of asteroids from meteorite data: Implications for magnetic anomaly detections. *Earth Moon and Planets*, 72:225–231.

Thomas, P. C., Veverka, J., Simonelli, D., Helfenstein, P., Carcich, B., Belton, M. J. S., Davies, M. E., and Chapman, C. (1994). The shape of Gaspra. *Icarus*, 107:23–29.

Uehara, M. and Nakamura, N. (2006). Experimental constraints on magnetic stability of chondrules and the paleomagnetic significance of dusty olivines. *Earth Planet. Sci. Lett.*, 250:292–305.

Wang, Z. and Kivelson, M. (1996). Asteroid interaction with solar wind. *J. Geophys. Res.*, 101:24479–24494.

Weiss, B. P., Berdahl, J. S., Elkins-Tanton, L., Stanley, S., Lima, E. A., and Carporzen, L. (2008). Magnetism on the Angrite Parent Body and the Early Differentiation of Planetesimals. *Science*, 322:713–715.

Weissman, P. R., Hicks, M. D., Abell, P. A., Choi, Y.-J., and Lowry, S. C. (2008). Rosetta target asteroid 2867 Šteins: An unusual E-type asteroid. *Meteoritics and Planetary Science*, 43:905–914.

Anlage M

Rosetta - ROMAP

To Planetary Science Archive Interface Control Document

RLGS-SPEC-SONC_DPS-SCIE-9065-CNES

RO-ROL-ROMAP-EAICD

Issue 1 Revision 3

13 March 2009

Prepared by: Instrument Archive Responsible and SONC

Approved by: Principal Investigator

IGEP
TU Braunschweig
Institut für Geophysik und extraterrestrische Physik

Distribution List

Recipient	Organisation

Change Log

Date	Sections Changed	Reasons for Change
2 March 2005	Creation of Issue 1 Revision 0	Initialized by TU-BS, updated by SONC. Delivered to DAWG.
24 May 2007	Sect. 2.2.1	Internal Review RIDs
14 January 2008	Revision 2	PI related RID's answered
16 March 2009	Revision 3 4.3.2, 4.3.5	Format of SPM levels 2 and 3 data changed to combined detached labels

TBD ITEMS

Section	Description
2.4.8	ROMAP-SPM Derived Data
3.4.3.6	Geometry directory

Table Of Contents

1 Introduction

1.1 Purpose and Scope

The purpose of this EAICD (Experimenter to Planetary Science Archive Interface Control Document) is two fold. First it provides users of the ROMAP instrument with detailed description of the product and a description of how it was generated, including data sources and destinations. Secondly, it is the official interface document between ROMAP and Planetary Science Archive (PSA) of ESA.

1.2 Archiving Authorities

The *Planetary Data System* Standard is used as archiving standard by:

- NASA for U.S. planetary missions, implemented by PDS
- ESA for European planetary missions, implemented by the Research and Scientific Support Department (RSSD) of ESA

ESA's *Planetary Science Archive* (PSA)
ESA implements an online science archive, the PSA

- to support and ease data ingestion
- to offer additional services to the scientific user community and science operations teams as e.g.:
  - o search queries that allow searches across instruments, missions and scientific disciplines
  - o several data delivery options as:
    - direct download of data products, linked files and data sets
    - ftp download of data products, linked files and data sets

  The PSA aims for online ingestion of logical archive volumes and will offer the creation of physical archive volumes on request.

1.3 Contents

This document describes the data flow of the ROMAP instrument on Rosetta from data acquisition until the insertion into the PSA for ESA. It includes information on how data were processed, formatted, labeled and uniquely identified. The document discusses general naming schemes for data volumes, data sets, data and label files. Standards used to generate the product are explained. Software that may be used to access the product is explained further on.

The design of the data set structure and the data product is given. Examples of these are given in the appendix.

1.4 Intended Readership

The staff of the archiving authority (Planetary Science Archive, ESA, RSSD, Lander team, design team) and any potential user of the ROMAP data.

1.5 Applicable Documents

AD 1. Planetary Data System Preparation Workbook, February 17, 1995, Version 3.1, JPL, D-7669, Part1
AD 2. Planetary Data System Standards Reference, June 1, 1999, Version 3.3, JPL, D-7669, Part 2
AD 3. Rosetta Archive Generation, Validation and Transfer Plan, January 10, 2006, Issue 2, Rev. 3, RO-EST-PL-5011
AD 4. ROSETTA Archive Conventions RO-EST-TN-3372 Issue 5, Rev. 0, 28 April 2009
AD 5. ROSETTA-RPC-MAG To Planetary Science Archive Interface Control Document EAICD RO-IGEP-TR0009 Issue 2.1
AD 6. ROMAP Electronics FM2 ADP, RO-LRO-DP-300002-UA, Issue 1, Revision 0, 16/05/2001
AD 7. ROMAP Boom & Sensor FM2 ADP, RO-LRO-DP-300003-UA, Issue 1, Revision 1, 16/07/.2001
AD 8. ROMAP Instrument Calibration Report FM2, RO-LRO-TR-300010-WM, Issue 1, Rev. 1, 15/11/2000
AD 9. CDMS Command and Data Management System - Subsystem Specification RO-LCD-SP-3101 29/08/2001, Issue 3, Rev. 5
AD 10. CDMS Command and Data Management System - Operation Manual RO-LCD-SW-3402 12/02/2001, Issue 1, Rev. 2
AD 11. Rosetta Time handling RO-EST-TN-3165, issue 1 rev 0, February 9, 2004
AD 12. DDID- Data Delivery Interface Document RO-ESC-IF-5003 Issue B6 23/10/2003

1.6 Acronyms and Abbreviations

CDMS	Command and Data Management System
CEM	Channel Electron Multiplier
CNES	Centre National d'Etudes Spatiales
CODMAC	Committee On Data Management, Archiving, and Computation
COSAC	Cometary Sampling And Composition
DDS	Data Delivery System (ESOC server)
DECW	Data Error Control Word
EAICD	Experiment Archive Interface Control Document
EGSE	Electronic Ground Support Equipment
ESA	European Space Agency
ESOC	European Space Operation Center
ESTEC	European Space Research and Technology Center
ESS	Electrical Support System
FM	Flight Model
FPGA	Field-Programmable Gate Array
GRM	Ground Reference Model
HK	Housekeeping
IWF	Institut für Weltraumforschung (IWF) in Graz
LOBT	Lander On Board Time
MPS	Max-Planck-Institut für Sonnensystemforschung
N/A	Not Applicable
NASA	National Aeronautics and Space Administration
OBDH	On Board Data Handling
OOBT	Orbiter On Board Time
OBT	On Board Time
PDS	Planetary Data System
PECW	Packet Error Control Word
PI	Principal Investigator
PID	Process Identifier
PSA	Planetary Science Archive
PVV	PSA Volume Verifier
SC	Science
QM	Qualification Model

ROMAP	Rosetta Magnetometer and Plasma Monitor
S/C	Spacecraft
SCET	Spacecraft Event Time
SFDU	Standard Formatted Data Unit
SONC	Science Operations and Navigation Center(CNES-Toulouse)
TBC	To Be Confirmed
TBD	To Be Defined
TC	Telecomand
UTC	Universal Time Coordinated

1.7 Contact Names and Addresses

Daniel Popescu, GFI Toulouse
data processing software responsible
dpopescu@gfi.fr

Hans Ulrich Auster, IGeP, TU-Braunschweig
Magnetometer PI
uli.auster@tu-bs.de
+49 531 391 5241

Istvan Apathy, KFKI Budapest
SPM PI
apathy@sunserv.kfki.hu
+36 209611030
+36 13922291

Gerhard Berghofer, IWF Graz
Controller responsible
Gerhard.Berghofer@oeaw.ac.at
+43 316 4120 564

Anatoly Remizov, IKI Moscow
SPM sensor responsible
remizov@linmpi.mpg.de
+49 5556 9790

Reinhard Roll, MPS Lindau
Pressure sensor responsible
roll@linmpi.mpg.de
+49 5556 979 166

2 Overview of Scientific Objectives, Instrument Design, Data Handling Process and Product Generation

Main scientific goals of ROMAP are (1) long term measurements on the surface to study the cometary activity as function of the distance from the Sun and (2) magnetic measurements during the descent phase of the Lander to investigate the structure of the remnant magnetization of the nucleus.
The ROMAP sensors (fluxgate magnetometer, electrostatic analyser and Faraday cup) measure the magnetic field from 0 to 32Hz, ions up to 8.0 keV and electrons up to 4.2 keV. High integration level of sensors and electronics. That is the basic for a combined field/plasma measurement instrument with less

than 1 Watt power consumption and 1 kg mass. Additional two pressure sensors are included in the ROMAP sensor arrangement. The sensors are moved from COSAC to ROMAP to optimise long term operation of pressure sensors. Data of both pressure sensors are transmitted within the housekeeping frame and are handled / archived as housekeeping values

2.1 Scientific Objectives

The Magnetometer (MAG) and the Simple Plasma Monitor (SPM) are the two experiments of the Small Instrument Package ROMAP, which complement the plasma packages onboard the ROSETTA Orbiter. Both instruments deliver data about the comet / solar wind interaction and the cometary activity as function of the distance from the sun and the onset of the diamagnetic cavity formation. The SPM sensor is able to determine the major solar wind parameters like density, speed, temperature, and flow direction. The Magnetometer sensor is able to determine the magnetic field vector.
Based on camera data from the flybys of the VEGA/GIOTTO spacecrafts at comet p/Halley in 1986, it was found that only a small part of the nucleus is active. As a consequence, new models about the internal structure of the nucleus were developed, in which the heat conductivity of the surface material is a key parameter. Up to the present, however, there are no direct measurements. On the background of such models, the gas production rate Q of the target comet p/Wirtanen was calculated as function of its radial distance to the Sun [Fuselier 1995; Kührt 1995]. Whereas the predictions of both models for perihelion distances are almost identical, they significantly differ for greater distances. For R=3.5AU, for example, there is a discrepancy of about four orders of magnitude: $Q=10^{23}\ s^{-1}$ according to Fuselier's model and $Q=10^{27}\ s^{-1}$ from Kührt. This great discrepancy is an example, which demonstrates the large uncertainties about the internal structure of the nucleus.
To date, most of the studies of comet-solar wind interaction address a well-developed cometary atmosphere. During the last decade, however, it has become apparent from both observation and theory that even weakly outgassing (or weakly magnetized) bodies may act as obstacles to the solar wind, creating effects that spacecraft magnetometers can resolve. As a result of bi-ion fluid simulations of the solar wind interaction with a weakly outgassing comet (Bogdanov et al. 1995), for example, one can distinguish between three main interaction regimes ordered with increasing neutral gas production rate Q. For $Q<10^{25}\ s^{-1}$ the cometary activity is negligible and the body behaves like an asteroid. In the range $10^{25}\ s^{-1} < Q < 10^{27}\ s^{-1}$ effects become important that cannot be explained in the framework of classical one-fluid MHD theory since the characteristic scale lengths are smaller than the heavy ion gyro-radius. There is no bow shock, only Mach cone-like structures, and the heavy ion fluid flows along a cycloidal orbit accompanied by a small-scale structuring (heavy ion bunching). This structuring is sensitive to the parameters involved (Alfven Mach number, plasma beta, production rate). In the range $10^{27}\ s^{-1} < Q$ one is confronted with a well-developed cometary atmosphere as, for example, found at p/Grigg-Skjellerup, p/Giacobini-Zinner and p/Halley. Characteristic features are the formation of a diamagnetic cavity in the immediate vicinity of the nucleus, a cometopause (ion composition boundary) and a bow shock.
For the formation of a magnetic cavity around the nucleus, from which the solar wind is excluded, a rough estimate can be derived. According to the momentum flux balance of solar wind and purely cometary plasma at the interface, the cavity radius is given by

$$R_{cavity} = \frac{\mu \sigma Q}{4\pi n_{sw} v_{sw}^2}$$

(σ ionisation rate, μ mass ratio cometary ions to protons, n_{sw} solar wind density, v_{sw} solar wind velocity; see also Haerendel 1987). A cavity with a radius of 10km (as a reasonable lower limit) requires a production rate $Q=5\times10^{27}\ s^{-1}$, which appears to be a threshold value for the existence of a cavity.
After landing, magnetometer and plasma monitor shall operate in a common mode (surface mode). Aim is to measure during a full cometary rotation period (8h). If the operation time is limited for energy reasons operation during a full cometary day (4h) is planed. The measurement shall be repeated in regular intervals (e.g. each 4 days) to monitor the plasma evolution with closer distance to Sun. Measurements have to be done synchronously with RPC onboard the orbiter.

For the first time ever, the ROSETTA mission will provide magnetic field measurements at very low distances from a cometary nucleus in a situation where the cometary activity is not yet fully developed. If the nucleus is not protected by an atmosphere produced by outgassing, the solar wind interacts directly with the intrinsic field and one can expect a situation similar to that observed at GALILEO's flyby at the asteroids Gaspra and Ida. Whereas the closest approach at these flybys was of the order of 1000 km, the situation here is much better because the surface field can be measured directly, practically not affected by the solar wind. In addition, during the approach to the nucleus, the probe can measure the variation of the magnetic field with distance and thus one should be able to clearly identify the type of the possible remnant magnetization.

Magnetometer data from GALILEO's flyby at the two asteroids Gaspra and Ida [Kivelson et al. 1993] together with model calculations [Baumgärtel et al. 1994, Kivelson et al. 1995a,b] have been interpreted in terms of an intrinsic magnetization of these bodies. It is generally assumed that this is remnant magnetization due to magnetic minerals such as iron-nickel, magnetite, and pyrrhotite, which were magnetized by relatively strong magnetic fields in the early solar nebula [e.g., Sugiura and Strangway 1988]. In the case of a generic relationship between asteroids and comets as to their refractory components, the magnetism of cometary nuclei could be caused by material exhibiting a natural remnant magnetization (NRM) in much the same way. Whether or not such material is present in cometary nuclei is still under debate.
Both, experimental results (mass spectrometry of particles escaped from p/Halley) and theoretical models point out primary magnetic minerals and possibly secondary magnetic material as well. One should expect the more pristine bright cometary regions to be characterized by rather primary magnetic material whereas the dark fractionated regions should be enriched by secondary magnetic material. More specifically, the following magnetic minerals/materials are being considered: $Fe_3 O_4$ (magnetite), Fe-Ni (metal) and $(Fe,Ni)_{0.9} S$ (pyrrhotite) as major carriers in the light regions and magnetite and a Fe-S-Ni-Si-O-rich phase in the dark regions. This is probably the main carrier of the NRM in bulk samples of C1-chondrites.

The growth of fractal aggregates from collisions between small dust grains is generally accepted to be the first step in the formation of planetesimals and cometesimals in the early solar system. Until now, the grain-grain interactions considered within this scenario were of mechanical and electrostatic nature only. If magnetized material were present at this stage, as is suggested by meteoritic and asteroidal evidence, magnetic interactions between dust particles should be taken into account as well. It has been shown experimentally [Nuth et al. 1994] and numerically [Nübold and Glassmeier 1999, 2000] that magnetized grains tend to build elongated structures of low fractal dimension and non-vanishing magnetic moment (see Figure 1). In case of enough magnetic material is available, this process may lead to centimetre or even metre sized magnetic structures, which ROMAP might be able to detect. Remnant magnetization of primitive objects such as comets could thus be called “accretional remanence”.

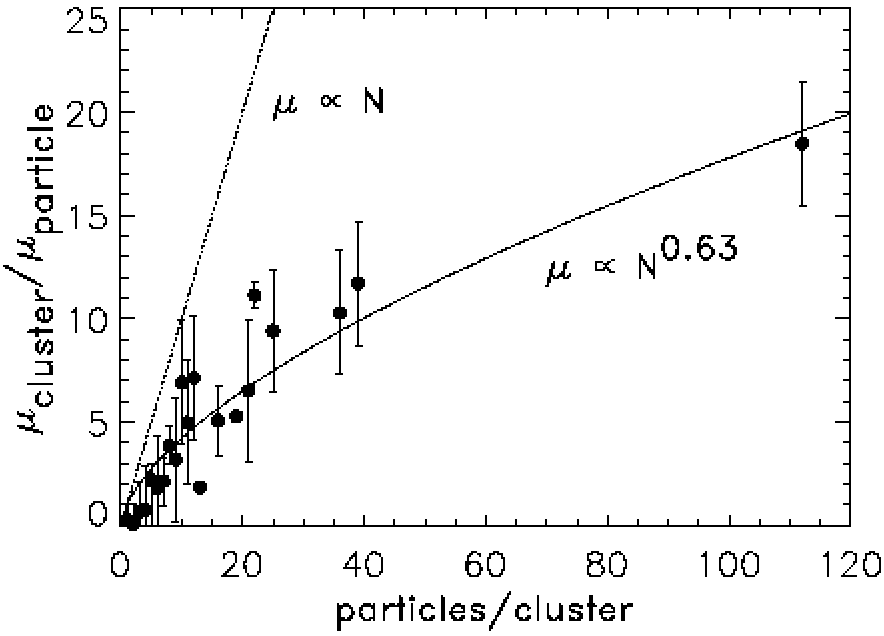

Figure 1 . Accretional remanence of growing magnetic dust aggregates in a numerical simulation [Nübold and Glassmeier, 2000].

2.2 Instrument Design

The ROMAP hardware consists of a combined magnetic field (MAG) and plasma (SPM) sensor mounted on a small boom, the near sensor electronics, a high-voltage generator (HV-part) and a small DPU (controller).

2.2.1 ROMAP Sensors

The magnetic field is measured with a vector compensated ringcore fluxgate magnetometer designed by the TU-Braunschweig and manufactured by the MPE Garching. The sensor consists of two ringcores (crossed in to each other) as well as pick-up coils and Helmholtz coils for each sensor axis. The coil system design without mechanical support allows the compensation of the external field on the ringcore position with high homogeneity and low weight (the overall sensor weight is 30g). Dynamic feedback fields as well as offset fields up to 2000nT can be generated in order to compensate Lander and/or Orbiter DC stray fields. The determination of Lander and Orbiter offsets could be done during the cruise phase using non compressible waves in the solar wind [Hedgecock 1975]. Parallel measurements of Lander and Orbiter magnetometer during Lander eject, descent and during measurement campaigns on the cometary surface will give an additional input for the inflight calibration.
The main part of the SPM-sensor is a hemispherical electrostatic analyzer with two channeltrons (CEM's) for ions measurement and one for electrons measurement. The entry of the ion channels is equipped with deflection plates to realize the spatial resolution. Despite the small size of the sensor, the sensitivity and resolution of the instrument are high and its field of view wide (appr. 100 degree). The E/q-range extends from 0 to 8 kV. Using CEMs in counting mode the electrostatic analyzer measures electron and ion distribution in a wide energy range. Hemispherical deflection plates analyze the energy in 32 or 64 steps. All major plasma parameters as electron-, proton and proton bulk velocity, density and isotropic temperature can be derived.
A retarding-grid Faraday cup sensor is implemented to measure currents due to fluxes of low energy charged particles on a collector plate. The Faraday cup measures the „reduced“ velocity distribution of the plasma due

to its inherent integration over velocities contained in a plane of differential thickness perpendicular to the axis of the sensor. Because the sensor is not differential in angle, the Faraday cup requires relatively low data rates. But for a given orientation it provides differential information in velocity space only along a direction perpendicular to the retarding grid [Lazarus et al. 1993].

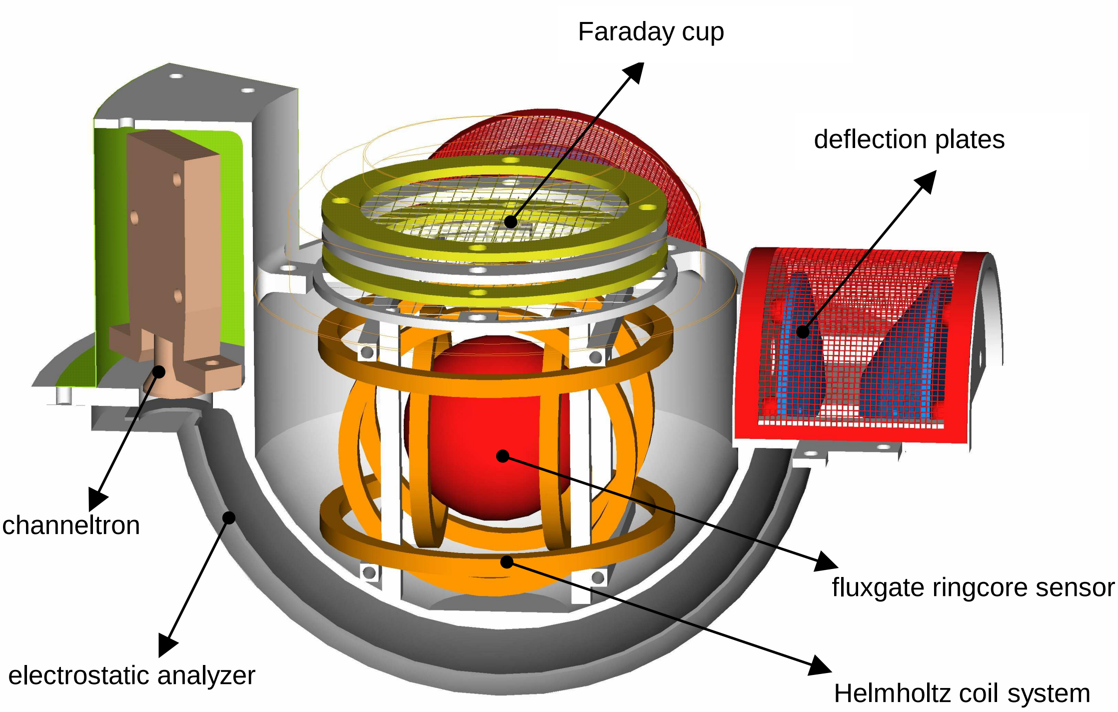

Figure 2 ROMAP MAG and SPM sensors compartment.

SPM sensor and fluxgate sensor integrated within one spherical sensor head. Figure 2 shows the sensor compartment. The sensor head is mounted on a 60 cm boom which is fixed with a hinge on the upper edge of the Lander structure and with a launch lock on the Lander balcony. After opening the launch lock, the boom will

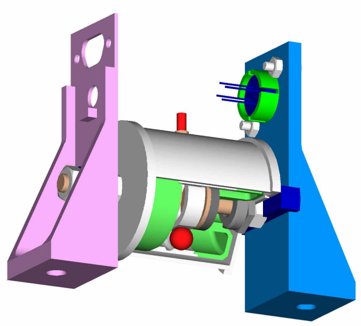

Figure 3 Pressure sensors

be deployed by two springs inside the hinge.

Two pressure sensors are selected to cover the whole pressure range from 10^{-8}mbar to 10^{1}mbar. For the range from 10^{-8}mbar to 10^{-3}mbar an ionising system (Penning) is deployed while for the range from 10^{-3}mbar to 10^{1}mbar a heat conduction sensor (Minipirani) is available. The pressure data are transmitted in the housekeeping frames. They are handled and archived as housekeeping and not as scientific values.
The combined magnetometer / SPM sensor is mounted on a 60 cm boom which is fixed with a hinge on the upper edge of the Lander structure and with a launch lock on the Lander balcony. After opening the launch lock, the boom will be deployed by two springs inside the hinge. Boom and the related coordinate systems are shown in Figure 4.

The SPM sensor, the Pressure sensors and all boom parts are designed by the MPS Lindau.

ROMAP sensor orientation

Coordinates (in Lander system) of rotation centre:

X:	186.82mm
Y:	-315.0mm
Z:	526.2mm

Sensor centre in stowed position:

X:	20.2mm
Y:	-315.0mm
Z:	58.7mm

Sensor centre in fully deployed position:

X:	-329.1mm
Y:	-315.0mm
Z:	526.2mm

Convertion of ROMAP system (R) in Lander System (L):

Stowed:

$$(L)=\begin{pmatrix} 0 & 0.336 & -0.942 \\ 1 & 0 & 0 \\ 0 & 0.942 & 0.336 \end{pmatrix}(R)$$

Deployed:

$$(L)=\begin{pmatrix} 0 & 1 & 0 \\ 1 & 0 & 0 \\ 0 & 0 & 1 \end{pmatrix}(R)$$

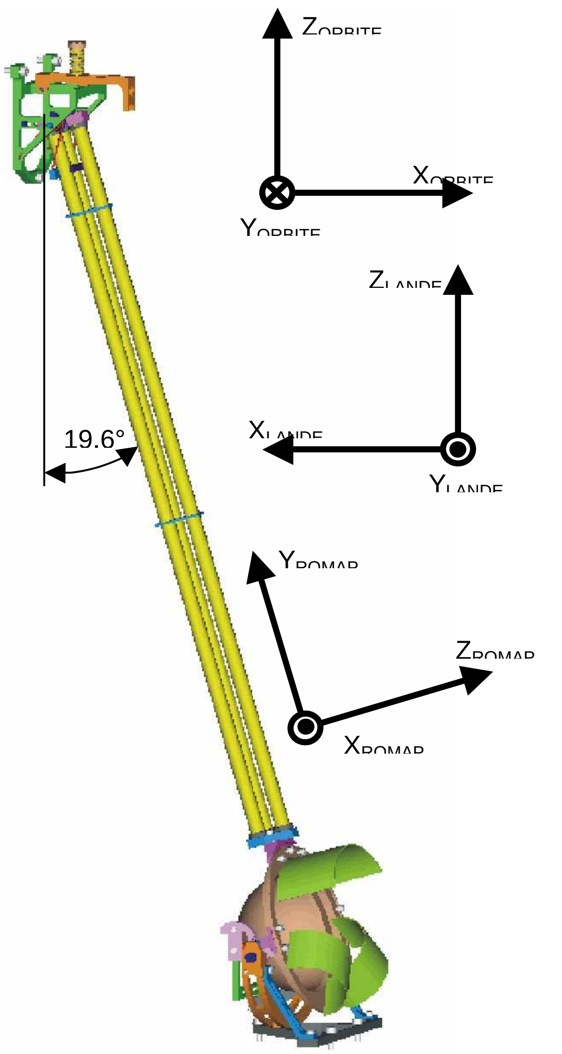

Figure 4 ROMAP sensors orientation

2.2.2 ROMAP Electronics

The ROMAP electronics consists of two boards placed inside the common electronics box. The central part of the near sensor electronics on the first board is a FPGA which controls AD and DA-converters. The 16-bit AD converters are digitising science and housekeeping data from all three sensors. In the block diagram (Figure 5) this data flow is drawn with dotted lines.

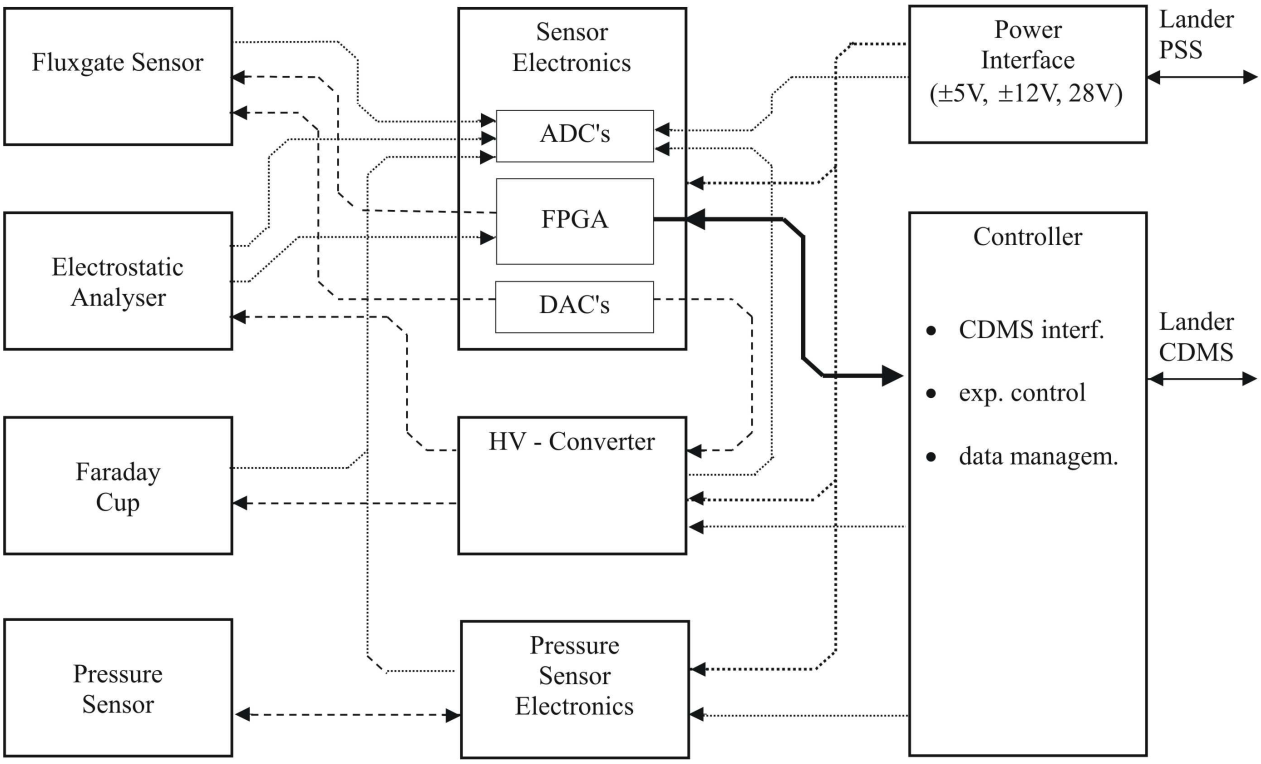

Figure 5 ROMAP electronics

Typical analogue parts of fluxgate magnetometers like filters or phase-sensitive integrators are substituted by fast digitalization of the sensor AC-signal and the following data processing in FPGA's (which overtakes the functions of the former analogue parts) [Auster et al. 1995]. In this way mass is saved without any loss of accuracy. The resolution is still restricted by sensor noise (less than 5pT/ √Hz at 1Hz) [Fornacon et al. 1999], not by electronics. Compensation fields for the magnetometer and high voltage steps for electrostatic analyser and Faraday cup are controlled via DA-converters (dashed lines). The near sensor electronics is developed by Magson GmbH Berlin The high voltage generator (developed by the KFKI) is in a separate shielded box on the front panel of the common electronics box..

The controller is located on the second ROMAP board. It controls MAG and SPM, stores their data output and implements the interface to the Lander Command and Data Management System (CDMS). It triggers the measurement cycle of the magnetometer, implements the digital magnetometer algorithm, controls the magnetometer feedback and generates data frames. For the SPM sensors the controller has implemented the counting logic for electrons and ions, samples Faraday cup data, generates SPM data frames, controls the high voltage parameters (energy, elevation), controls the channeltron HV-supply and computes the plasma parameters. In the parameter mode only the sums of the rows and columns of the sampled ion and ion-current arrays are transmitted. The controller is based on a RTX2010. Address decoder, reset logic, clock generators, control signals generator, watchdog logic and CDMS interface are integrated within a FPGA. Hard- and software are developed by the IWF Graz.
The instrument parameters and the required recourses are given in the following tables:

Instrument parameters:

type of sensor	***parameter***		***value***
Fluxgate Magnetometer	dynamic range resolution sensor noise frequency range offset drift		±2.000nT 10pT <5pT/√Hz 0...32Hz <0.1nT/℃
Electrostatic, Hemispherical Analyzer	channels energy range field of view energy steps max. count rate exposition time	ions electrons ions electrons ions electrons	2 CEM 1 CEM 40 ... 8000eV 0,35 ... 4200eV 100°x 100° 10°x 60° 32 or 64, log. scaled 10^6 counts/s 40 ... 1.000ms
Faraday cup	ion integral energy distribution resolution (current mode) field of view energy steps entrance area		up to 2000 eV ±1.5 10^{-12} - ±5.10^{-10} A 140^0 x 140^0 16 steps 6 cm^2
Penning Sensor	range electric Field magnetic field		10^{-8} – 10^{-3}mbar 10^6 V/m 700 Gauss
Pirani Sensor	range bridge resistors		10^{-3} – 10 mbar 1kOhm

ROMAP Resources

recourses	***experiment part***	***requirements***	Σ
mass	MAG sensor	40g	
	SPM sensor	120g	
	Pressure sensor	110g	
	boom + hinge + cable	80g	
	launch lock	40g	
	pressure harness	50g	
	electronics in CEB (interface, analogue, controller, HV-box, connectors, frontplate)	360g	
	Pressure E-Box	130g	930g
power	sensor electronics	350...550mW	
	controller	180mW	
	penning electronics	100mW	
	pirani electronics	50mW	
	HV-part	200mW	<900mW
telemetry rate	surface mode MAG SPM	 70 bits/s 30 bits/s	 80 bits/s
	slow mode MAG	 70 bits/s	 68 bits/s
	fast mode MAG	 4400 bits/s	 4369 bits/s